SOURCE ROCK EVALUATION OF GORU SHALES, GAMBAT LATIF BLOCK, SOUTHERN INDUS BASIN, PAKISTAN

By

AQSA IJAZ

DEPARTMENT OF EARTH SCIENCES

QUAID-E-AZAM UNIVERSITY, ISLAMABAD

2022

SOURCE ROCK EVALUATION OF GORU SHALES, GAMBAT LATIF BLOCK, SOUTHERN INDUS BASIN, PAKISTAN

A thesis submitted to Quaid-e-Azam University, Islamabad in partial fulfillment of the requirement for the degree of MPhil in Geophysics

AQSA IJAZ

DEPARTMENT OF EARTH SCIENCES

QUAID-E-AZAM UNIVERSITY, ISLAMABAD

2022

ABSTRACT

With the increase in energy demand around the globe, hydrocarbons resources are depleting around the globe at a spiking level. Aside from conventional reservoirs, a significant amount of hydrocarbons are trapped in unconventional reservoirs. Concentration of TOC and kerogen maturation level play the key role in determining the ability of organic rich shale formation to act as a potential source rock. Our study area is Tajjal Gas field in Gambat-Latif Block which lies in Southern Indus Basin. The Gambat-Latif Block lies in extensional regime hence normal faults are found in the region. Lower Goru is the most prospective formation in the area which comprises of thin interbedded shales and sandstones and these beds act as source rock and reservoir respectively. For source rock characterization; along with seismic interpretation and well log analysis, seismic inversion and neural network method is utilized. Structural interpretation of 3D seismic data includes marking horizons, fault geometry mapping, and time and depth structural maps of Lower Goru and its sand units**.** The time contour map of B-Sand Interval shows that zone of interest is extending in the eastward direction. For source rock evaluation, TOC is computed using well logs. B-Sand Interval in wells Tajjal-02 and Tajjal-03 shows source rock properties with an evaluated average TOC of 1.2-2.5 wt. % and 0.2-1.5 wt. % respectively. For the impedance prediction of B-Interval, post stack inversion technique i.e. linear programming sparse spike inversion has been applied which resolves the low impedance zone in Tajjal-02 and Tajjal-03 and provides the acoustic impedance distribution across the area. Organic matter is marked by low velocity and density as compared to surrounding rock hence seismic attributes like P- impedance would respond to high "TOC" content. For computation of TOC across the study area, TOC data is superimposed and interpolated on impedance blocks using neural networks. The model created using neural network indicates an average TOC ~2.6 wt. % at Tajjal-02 and its surroundings and approximately ~0.5 wt. % in the vicinity of Tajjal-03. Such characteristics indicate that B-Sand interval possesses poor to fair source generation potential.

DEDICATION

I dedicate this research work to my beloved parents.

ACKNOWLEDGEMENTS

I am very much grateful to Allah Almighty with whom blessings, I have been able to complete my research work.

I am highly thankful to my supervisor, **Dr. Tahir Azeem**; Assistant Professor at Department of Earth Sciences, Quaid-e-Azam University, Islamabad, for his academic guidance and support whenever I needed it. I am really appreciative of the assistance and help that he extended towards me.

I am extremely grateful to Mr. Zahid; petrophysicist at MPCL and Miss Faryal Mehmood, assistant geophysicist at MPCL for their guidance at all stages of this work. Their contribution and guidance is the main driving force in completion of this research work.

I cannot forget to thank my friends, Abdul Moiz for all his help and contribution at some stage of this work. His help is of vital importance for successful completion of this work. Last but not the least, I am highly indebted to my parents for their immense support in every thick and thin of my life and especially throughout this research. May ALLAH bless them in every single aspects of their lives. Ameen.

TABLE OF CONTENTS

TABLE OF FIGURES

TABLE OF TABLES

CHAPTER 1
INTRODUCTION

1.1. INTRODUCTION

Energy sources have a huge significance in the economic growth of any country, the demand for which increases with the increase in population (EIA, 2013). Since the first exploration of hydrocarbons in early middle of 20th century, they have quickly become a vital energy resource around the globe and have played a significant role in turning the world to a global village. Generally, the oil/gas is explored and extracted from the reservoir rock i.e. sandstone and limestone (faulted or porous) which have high porosity and permeability. Reservoir rock is overlain and underlain by low-permeability formations/layers i.e. seal and source rock which trap the hydrocarbons in reservoir rock. With the increase in energy demand around the globe, hydrocarbons resources are depleting around the globe at a spiking level. This has led to unconventional hydrocarbon exploration i.e. from low-permeability formations/layers. If shales and mudstones have a significant quantity of organic content, they are classified as source rock (Passey et al., 1990). Aside from conventional reservoirs, a significant amount of hydrocarbons are trapped in unconventional reservoirs i.e. tight gas, coal bed methane and shale oil/gas. Shale oil/gas is one of the types of unconventional reservoirs (Sunjay, 2011).

As Pakistan has the 6th largest population in the world, natural hydrocarbon resources are depleting at a significant rate as reported by SDPI (Sustainable Development Policy Institute) hence there is an urgent need to explore unconventional hydrocarbon resources to meet the energy demands (Abbasi et al., 2014). More than 827,365 km^2 of Pakistan's land comprises of sedimentary basins which comprise of thick successions of shale formation as a source and have good petroleum systems. In recent years, Indus Basin of Pakistan is broadly studied for the evaluation of unconventional hydrocarbon potential (Ziagham and Mallick, 2000). Shale gas makes up approximately 70% of the sedimentary basins in Pakistan with nearly 200 trillion cubic feet (TCF) of unconventional resources within the shale formations. According to EIA (Energy Information Administration), Pakistan has total of 586 TCF shale gas reserves, however 100-105 TCF are the recoverable shale gas resources (EIA, 2013).

Lower Goru shales, Sembar and Ranikot formations are the major potential sources of Indus basin and has shale gas ranging from 180-210 TCF (Abbasi et al., 2014).

About a decade ago, E&P sector had limited interest in the characterization of source rock using seismic rock properties. However, after a decade of tremendous advancement in technology and softwares which have resulted in frequent use of drilling techniques such as horizontal drilling and hydraulic fracturing, source rocks are now also being studied and treated as reservoir lithologies.

The key factors for the classification of source rock are level of organic maturity (LOM), total organic content (TOC) and viterinite reflectance (Ro) (Welte and Tissot, 1984; Peters and Cassa, 1994). Concentration of TOC and kerogen maturity level are the primary constituents to determine the ability of an organic shale to contain and potentially produce hydrocarbon (Tissot and Welte, 1978). For a shale and limestone formation to classify as a source rock, they need to contain ~1% organic matter or at least 0.5% TOC. Organic rich source rocks have been observed around the world with as much as 10% TOC. TOC influences log response in source rocks. Presence of organic content results in low density, lower sonic transit time and higher resistivity on petro logs. Density log is used for the estimation of TOC and TOM (total organic matter) by following the techniques proposed by Myers and Jenkyns (1992) and Schmoker and Hester (1989).

Petro elastic properties play a significant role in the identification of possible drilling zones of shale gas/oil (Ali et al., 2017). Presence of organic matter may also affect the petro elastic properties in shale rocks i.e. low permeability (K), high brittleness index (B) and moderate Young's modulus € is favorable for hydraulic fracking and drilling of shale oil/gas zones.

Not all shale formations act as source rock and hydrocarbon producer. Clay content, primary and secondary porosity and most importantly, the presence of kerogen content in shale formation results in heterogeneity and anisotropy. Organic mudrocks are generally recognized as dark-gray to black colored ultra-fine grains with dispersed-organic-matter content hence they are not the ideal candidates for standard quantitative petrography. Elastic properties of shales also vary due to presence of different minerals (aspect ratio and composition) i.e. Quartz, silica, carbonates and clays as observed in multiple XRD analyses.

1.2. LOCATION AND PHYSIOGRAPHY

Gambat-Latif Block is located in Sindh province, about 120 km south-east of Sukkur in district Sanghar. It lies in Southern Indus Basin of Pakistan constituting almost 3648.73 square kilometers of area. Tajjal gas field is producing field on Gambat Block having coordinates 26˚ 52' 50" N & 68˚ 55' 60" E with an altitude of 45 meters above sea level. Sawan gas field and Miano gas field are the nearby prominent gas fields surrounded the Tajjal gas field.

Gambat-Latif block lies in the Nara Desert which mainly contains farmland and marshy areas but thirty percent of the project area is cultivated with help of Nara Canal. 3D survey of Gambat-Latif has an extension of 675 square kilometers and a cube of 10 kilometers has been awarded to complete this dissertation.

Figure 1.1. Location of Gambat-Latif Block and major petroleum fields in Pakistan (www.ppl.com.pk).

1.3. EXPLORATION HISTORY OF STUDY AREA

Pakistan Petroleum Limited (PPL) and OMV Pakistan started the exploration activities in the project area in the early 21st century as a joint venture. By the mid of first decade of 21st century exploration parties had acquired extensive concession blocks. OMV (35%), ENI (30%), PPL (30%) AND GHPL (5%) are the operating partners in the Gambat-Latif block. OMV conducted extensive seismic survey in and around the block along with a mega 3D covering more than 1000 square kilometers of the area.

By year 2007, Tajjal-01 well came as a producing well during testing and enhanced further exploratory projects in the adjacent areas. Appraisal wells Tajjal-02 and Tajjal-03 were left as dry holes. Though initially, Tajjal-04 produced gas but later on it began producing large quantity of water with sand hence production was ceased from the well. Producing field is Tajjal gas field recoverable reserves are 19Bcf. Current daily gas volumes are 0.57mmscf (https://www.ppl.com.pk/). Figure 1.2 shows area of interest in Gambat-Latif Block (LMKR). Different geometric figure are showing Blocks which are demarcated by DGPC whereas small blue circle show the wells. Our area of study is located in Gambat-Latif Block.

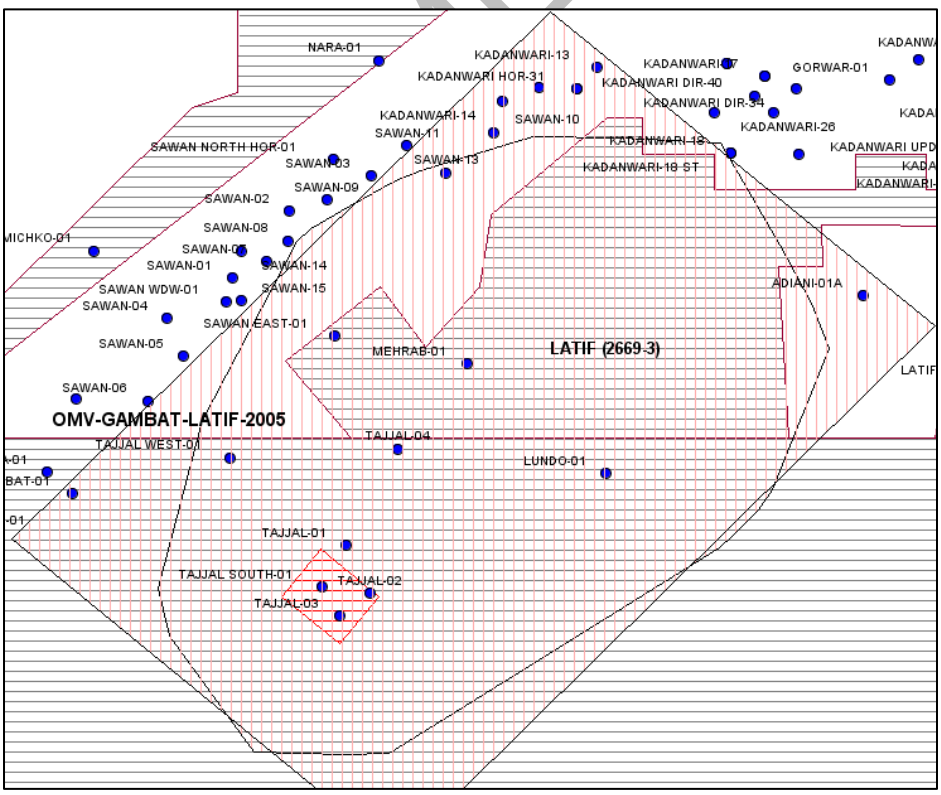

Figure 1.2. Map showing area of interest in Gambat-Latif Block with surrounding fields in Southern Indus Basin (LMKR).

1.4. AVAILABLE DATA

For this research work, a 3D seismic cube of 10 square kilometers of area along with well log data of 3 wells; Tajjal south-01, Tajjal -02, Tajjal-03 were provided by LMKR after approval from DGPC.

1.5. METHODOLGY

The following methodology was adopted to carrying out this research project:

1) QC of seismic and well data
2) Generation of synthetic seismogram
3) Marking of faults
4) Horizon picking on seismic data
5) Generation of time and depth structural maps for every marked horizon
6) Source rock evaluation using well data
7) Seismic inversion
8) TOC computation across the 3-D area using Emerge

The software used for this research work are Kingdom, Techlog and Hampson Russell.

1.6. OBJECTIVE

The objective of this research work is to identify the source rock potential of Lower Goru Formation in Gambat-Latif Block. Goru Formation comprises of interbedded shale and sandstone layers. The shale layers of Lower Goru Formation are studied to identify any potential source rock characteristics in it.

CHAPTER 2

TECTONIC SETTING AND GENERAL GEOLOGY

2.1. TECTONIC SETTING

Pakistan has of two major sedimentary basins i.e. Balochistan and Indus Basin. Different geological events and settings resulted in the development of these basins which later on joined together along the Ornach-Nal/Chaman Strike Slip fault during Cretaceous/Paleocene age. Indus Basin is the largest onshore basin in Pakistan covering most of the eastern part of Pakistan and western part of India with an aerial extent of about 873000 square kilometers. In our part of the region, Indus Basin is further divided into Upper, Central and Southern Indus Basin, on the basis of their petroleum prospects and structural regime (Naeem et al., 2016).

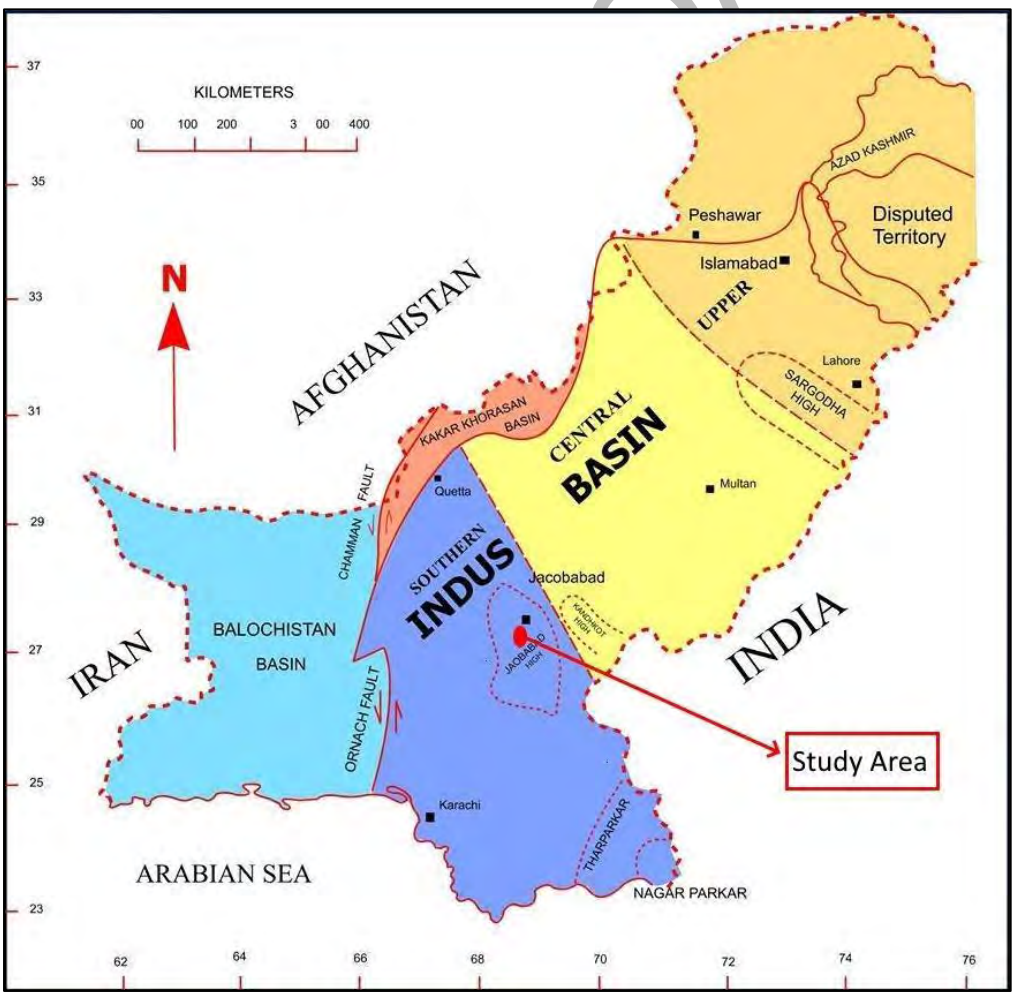

Figure 2.1. Tectonic map of Pakistan along with location of Gambat-Latif Block (Farah, A et al., 1984).

Gambat-Latif block lies in the Southern Indus basin which lies in extensional regime. As Indian plate diverged from Gondwanaland in late Jurassic period, major structural and stratigraphic features of Southern Indus Basin developed. As Indian plate continued its movement towards north in late Cretaceous, flysch gathered around the southern rim of the Indian plate. As the Tethyan Sea closed due to convergence, Sulaiman-Kirthar fold belt formed along the colliding edge of Indian plate (Sheikh et al., 2017).

Central Indus basin and Southern Indus basin are separated by Sukkur rift comprising of Khairpur-Jacobabad and Mari-Kandhkot high. Southern Indus basin is enclosed by the Sukkur rift on the north, axial belt to the west; Indian shield to the east; and by Arabian Sea on the south. Southern Indus basin consist of five main units, the Thar Platform, Karachi Trough, Kirthar Fore-deep, Kirthar Fold Belt and offshore Indus. Thar Platform is gently sloping monocline, surrounded by Indian shield in the east. Figure 2.1 (Khalid et al., 2018) and 2.2 (Brohi et al., 2013) show the area of interest on Thar Platform in tectonic map of Pakistan and Lower Indus Basin respectively. Karachi trough is an embayment opening up into the Arabian Sea. Kirthar Fold Belt is a north-south trending tectonic feature. Kirthar Fore-deep is north-south oriented area of subsidence. Offshore Indus is an area forms the part of passive continental margin (Kadri, 1995).

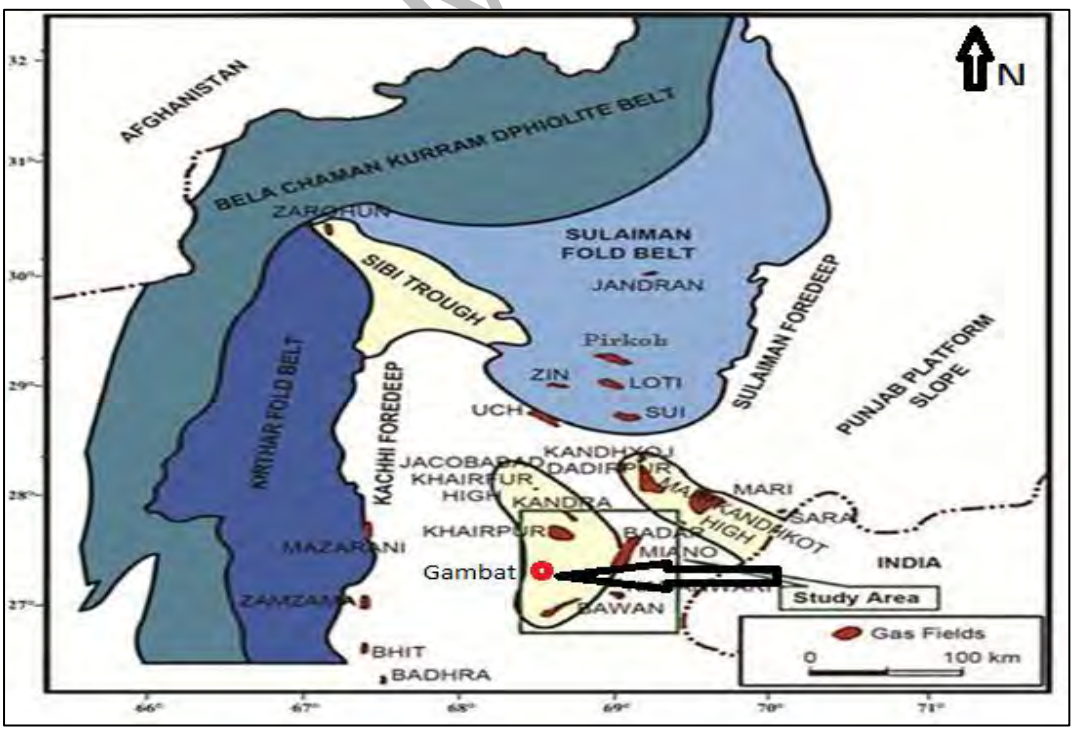

Figure 2.2. Tectonic map of Southern Indus Basin along with location of Gambat-Latif Block (Farah, A et al., 1984).

2.2. GENERAL GEOLOGY

Tajjal gas field (Gambat-Latif Block) is situated in Southern Indus Basin. It is surrounded by Panno-Aqil sub basin in north, Kirthar sub basin in south, by Indian shield in east and by the Kirthar fold belt in the west (Ahmed et al., 2007). Southern Indus Basin was formed as a part of large scale extensional regime hence normal faults and related horst and graben structures are widely distributed which were mostly formed during divergence during Cretaceous time; at the time of deposition of main source and reservoir rocks of Southern Indus Basin. Later the anticlockwise rotation of Indian plate further complexed the already existing extensional structures. This region is characterized by both structural, stratigraphic and their combination traps (Ahmed et al., 2010).

2.3. PETROLEUM SYSTEM OF SOUTHERN INDUS BASIN

The oldest formation encountered in Southern Indus Basin is Wulgai Formation of Triassic age to the youngest formation being Siwaliks of Pliestocene as shown in Figure 2.3 (Siyar et al., 2017). A major unconformity is also marked between Jurassic carbonates and lower most Cretaceous clastic sediments (Sembar Formation) (Kadri, 1995).

Southern Indus basin produces 37% hydrocarbons in Pakistan (Kadri, 1995). Tajjal South-01 well was drilled down to the level of Lower Goru A-Interval of Cretaceous formation, while other two wells were drilled down to the level of Lower Goru B-Interval of Cretaceous formation. Table 2.1 shows the stratigraphic column of wells in study area.

2.3.1. Source

On the basis of TOC, thermal maturity and type II/III oil-prone kerogen, early Cretaceous Sembar Formation acts as the major proven petroleum source rock in the basin. It mainly constitutes of silty black shale along with significant content of sandstone, siltstone and minor interbedded nodular limestone. In the western and north-western part of basin silt, shale and marl are the main constituents of this thermally matured, open marine source rock whereas sandstone covers the south-eastern and eastern part of the basin where the formation thins out (sheikh et al., 2017).

Along with Sembar Formation, Lower Goru Formation shale beds and Paleocene Ranikot Formation also act as source rock in some places. The moderately organic shale rich

C-Sand and B-Sand intervals of Lower Goru Formation have fair to good genetic source potential (Qadri, 1995).

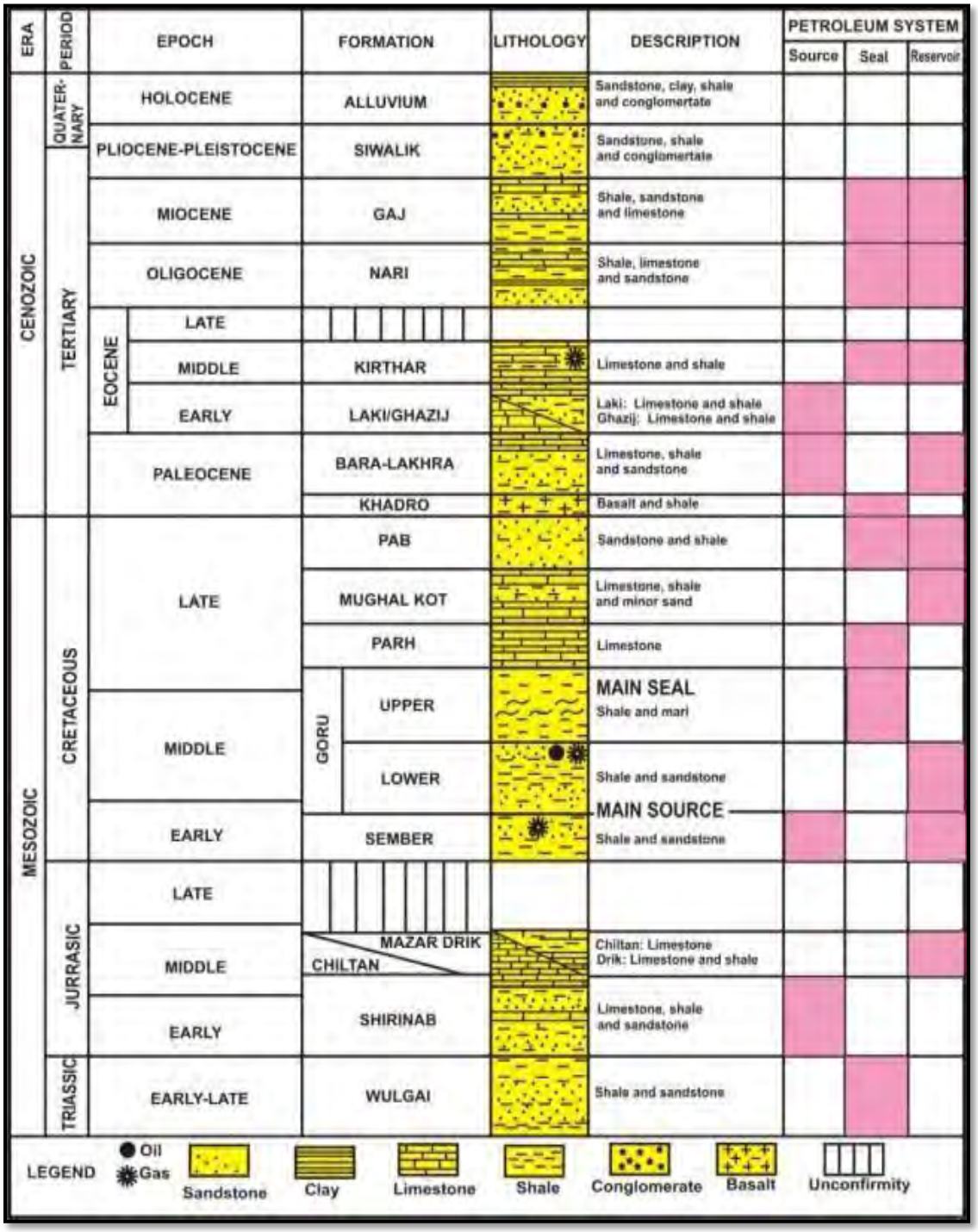

Figure 2.3. . Generalized stratigraphy of Southern Indus Basin (Siyar et al., 2017).

Table 2.1: Stratigraphic column for wells under study.

AGE	FORMATION	TAJJAL SOUTH-01 (m)	TAJJAL-02 (m)	TAJJAL -03 (m)
Recent Miocene	Alluvium-Siwalik	164.00	151.00	147.00
Eocene	Drazinda Member	37.00	0.000	0.00
Eocene	Kirthar Member		54.00	51.00
Eocene	Pirkoh Member	4.00	60.00	59.00
Eocene	Sirki Member	293.00	167.00	128.00
Eocene	Habib Rahi Member	38.00	177.00	197.00
Eocene	Laki		0.00	687.00
Eocene	Ghazij Member	730.00	695.00	0.00
Eocene	Sui Main Limestone Member	110.00	101.00	102.00
Paleocene	Ranikot	1168.00	1134.00	1198.00
Late Cretaceous	Upper Goru	400.00	403.500	0.00
Cretaceous	Goru			361.00
Lower Cretaceous	Shale Interval	0.00	0.00	0.00
Early Cretaceous	Lower Goru		327.50	521.00
Lower Cretaceous	B Interval	190.00	219.500	129.00
Lower Cretaceous	D Interval	45.00	39.50	32.00
Lower Cretaceous	C Interval	166.00	307.00	188.00
Lower Cretaceous	A interval	173.00		

2.3.2. Reservoir

In Southern Indus Basin, Lower Goru Formation of Cretaceous age is deposited in shallow marine setting comprising of medium to coarse sandstone and acts as the major proven reservoir rock (Naseer et al., 2016). Basal sands of Lower Goru Formation are divided from top to bottom into D- Sand, C- Sand, B-Sand and A- Sand intervals respectively (Ahmed et al., 2010) as shown in Figure 2.4. B- Sand Interval acts as the major oil and gas producing reservoir rock unit in the Gambat Block. Average porosities are about 11% in the prospect area.

2.3.3. Seal

To restrict the hydrocarbon within the reservoir a barrier must be present. In Southern Indus basin for Sembar-Goru petroleum play, marl and silt stratigraphic sequences of the Upper Goru Formation act as the major seal rock (Kazmi & Abbasi, 2008). Transgressive shales of Sembar Formation and Ranikot Formation can also act as seal. In the Lower Goru reservoir sometimes the thin layers of shale can also act as better seal for hydrocarbon accumulation (Naeem et al., 2016).

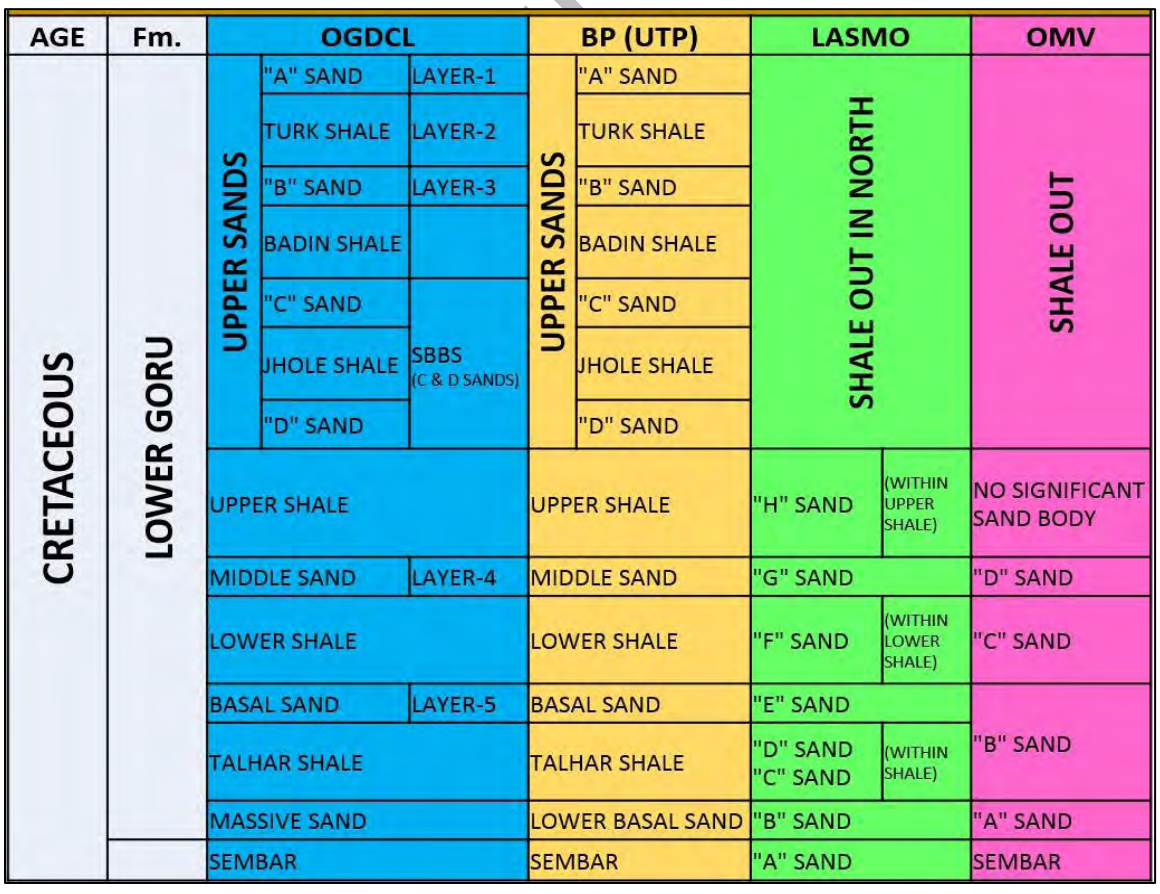

Figure 2.4. Nomenclature of Lower Goru sand units used by different companies.

2.3.4. Trapping Mechanism

Southern Indus Basin was formed as a part of large scale extensional regime hence normal faults and related horst and graben structures are widely distributed which were mostly formed during divergence during Cretaceous time; at the time of deposition of main source and reservoir rocks of Southern Indus Basin. Later the anticlockwise rotation of Indian plate further complexed the already existing extensional structures. This region is characterized by both structural, stratigraphic and their combination traps (Ahmed et al., 2010).

2.4. STRUCTURAL SETTING OF GAMBAT-LATIF BLOCK

Gambat-Latif Block is located in the extensional regime hence it is highly marked with normal faults and related horst and graben structures as shown in Figure 2.5. It oldest formation encountered is of Cretaceous age while the Paleocene Siwaliks form the youngest formation observed. The Lower Goru formation consists of sand intervals i.e. D, C, B and A Intervals respectively. The Lower Goru formation is dipping towards west and trending SE-NW (Kazmi & Abbasi, 2008). From the kitchen in Sembar formation, fault planes migrate the hydrocarbons to the reservoir rocks. As no outcrop is found over the study area, seismic interpretation is the only source for structural interpretation.

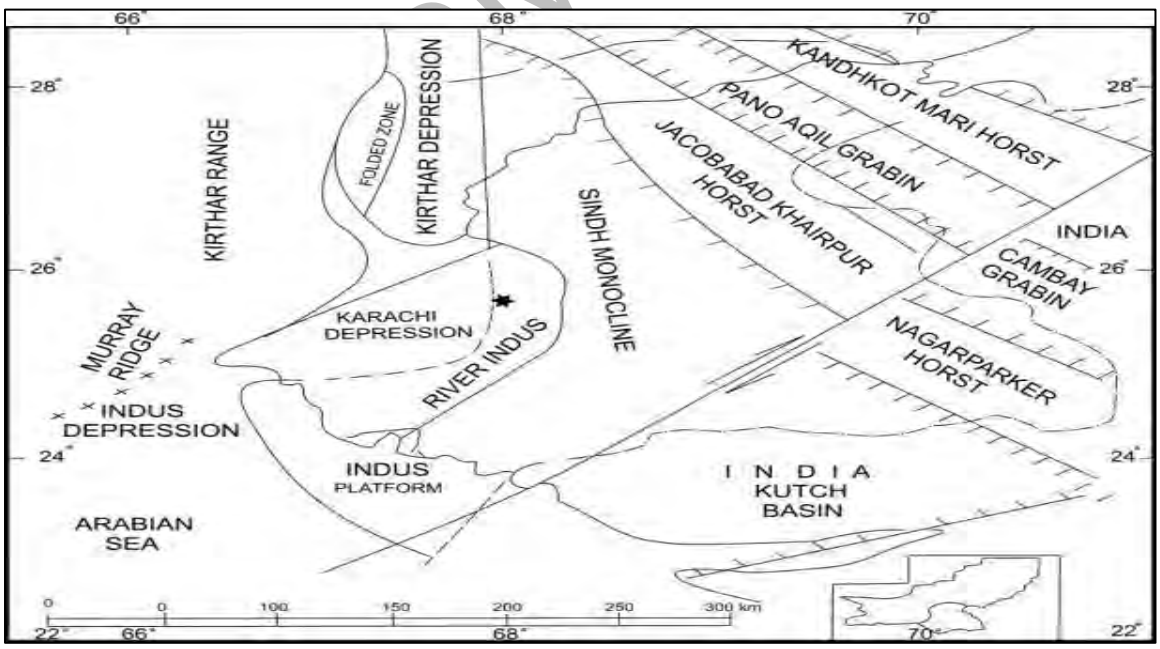

Figure 2.5. Tectonic map of Southern Indus Basin (Brohi et al., 2013).

CHAPTER 3
INTERPRETATION OF 3D SEISMIC DATA

After improving signal to noise ration during processing on acquired seismic data, the seismic section is worth interpreting and thus subsurface geological structures can be deduced from it. Seismic interpretation involves using different techniques of data correction, migration and time depth conversion to produce a structural image from seismic reflected data. (Dobrin and Savit, 1960) .

Seismic interpretation initiates by mapping the large scale subsurface structures in the area, i.e. fault planes and marking horizons. Horizons are generally marked on strong reflectors on seismic sections which can be easily followed over the seismic data. Sequence boundaries and top of reservoir are important horizons to be marked as they along with marking geological age can also help in identifying stratigraphic traps. Faults are marked on discontinuity, displacement and distortion in horizons. To mark faults and to be able to continue a horizon over a fault; along with knowing the type of faults in the region, the interpreter needs to identify the amount of vertical displacement of horizons along the faults. It may be possible that one reflector seamlessly continues over a fault into a different reflector (Bakker, 2002).

Seismic data is a subsurface image and interpretation leads to understand subsurface structures and stratigraphy. By means of this interpretation, interpreter moves forward to the analysis of target like minerals and hydrocarbons, reservoir, earthquakes study and engineering purposes etc.

Structural and stratigraphic analysis are made based on interpretation of seismic data. Structural analysis is used to search for structural traps which could possibly host hydrocarbons such as anticline, dome, horst and graben, flower structure, pop-up structures, growth faults, imbricate and duplex structures. Strong reflectors are marked as horizon which show a significant change in lithology hence stronger reflection of seismic waves. Subsurface geometry of selected reflectors is studied using time and depth structure contour maps (Coffeen, 1986).

Sequences of reflections are identified and marked on seismic data which are interpreted as the seismic expression of sedimentary sequences. Stratigraphical analysis is done

mostly in extensional regime because due to extensive tectonic activity in compressional regime resulting in faulting, mountain building and in some cases metamorphism of rocks, it's difficult to mark the continuity of reflectors (Coffeen, 1986).

3.1. STRUCTURAL ANALYSIS

Structural analysis comprises of identifying and marking possible faults and horizons on seismic data to investigate and identify potential hydrocarbon accumulation zones. These potential zones are marked on the bases of age, formation and structures such as anticlines and faults which are able to accumulate and preserve the hydrocarbons over millions of years (Coffeen, 1986).

As seismic data is on time scale, two-way-travel time is mostly used for structural interpretation. This seismic time domain data is then converted to depth domain which show the possible depth of geometric features. The accuracy of depth depends on the accuracy of certain data like velocities of the area that is obtained from the check shot or vertical seismic profile surveys. These surveys give us time versus depth relation from which velocity can be calculated.

Firstly the faults are interpreted on time sections. Faults are correlated with each other by making polygons that show certain structure and then on these time faults, horizons are marked which indicate the beddings i.e. from where there is certain change in lithology. From these fault and horizon interpretation on time sections we get TWT time maps. These maps are very helpful in the indication of structural traps, the orientation of faults and their geometries.

3.2. BASIC WORK FLOW OF SEISMIC INTERPRETATION

Following are the major interpretation steps that are taken to interpret the seismic date:

1. Area base map preparation
2. Fault picking on seismic section
3. Synthetic Seismogram generation
4. Horizon Interpretation
5. Construction of fault polygons
6. Creation of time and depth structural maps

3.2.1. Area Base Map Preparation

Base map is a map prepared when the geographic coordinates of study area are loaded in the Kingdom software along with primary well and seismic data and interpretations can be plotted. The seismic data may be 2D or 3D. The 2D data comprises of dip and strike lines which are acquired individually according to the structure of the area, as opposed to the multiple closely spaced orthogonal inlines and crosslines in the form of cube that constitutes 3D data. The wells in the study area are loaded and displayed on the base map. Figure 3.1 shows the cubic base map with 3D seismic data and three wells.

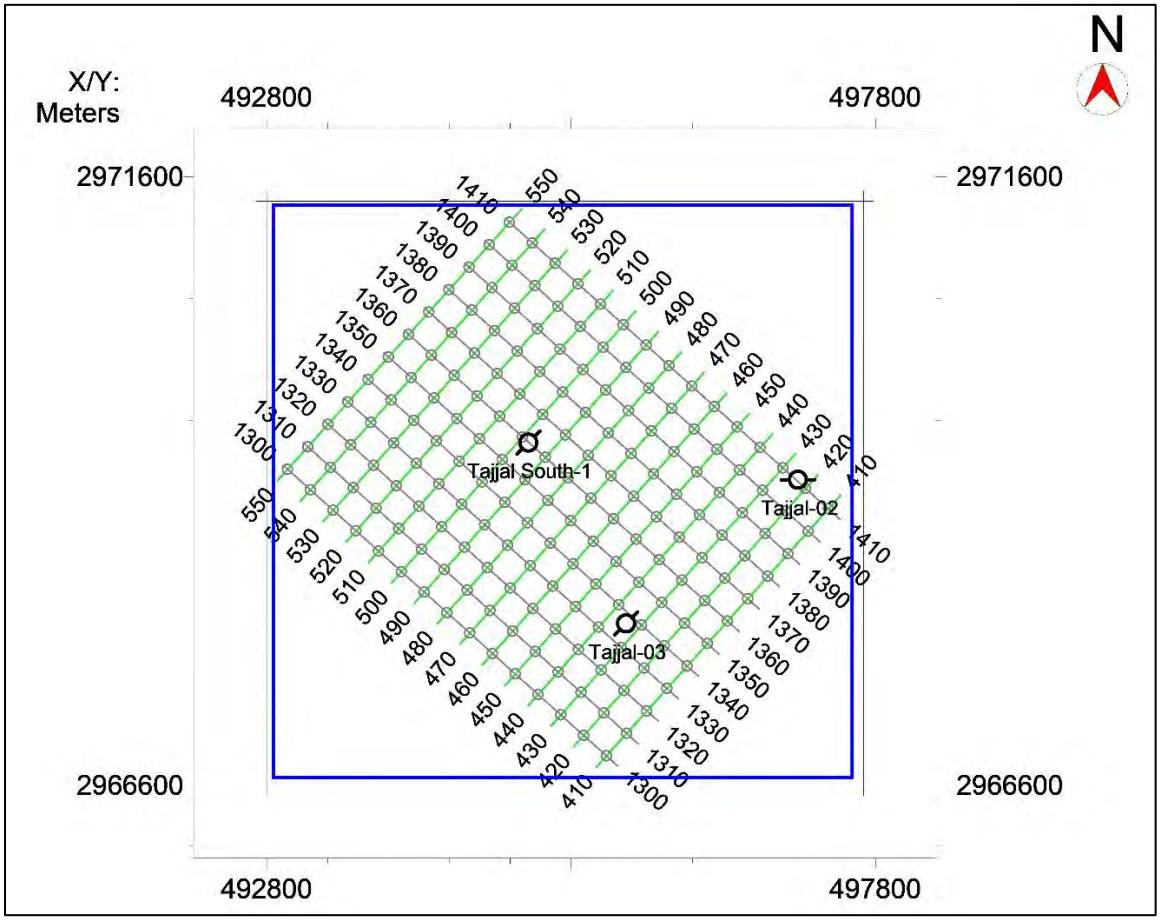

Figure 3.1. Base map of Gambat -Latif Block presenting 3-D geometry of inlines and crosslines along with three wells.

3.2.2. Fault Picking on Seismic Section

Faults are interpreted on seismic data where there is certain discontinuity or breakage in the beddings. The first step in seismic data interpretation was the identification of faults in seismic data. On basis of prior geological and geodynamic information of study area, faults

were identified by discontinuities observed and by seeing a significant displacement in the seismic reflectors. The pattern of the faults is identified by the prior knowledge of the stress regime i.e. compressional and extensional. Mostly in compressional regime reverse faults are dominant with minor normal faults but in extensional regime we observe normal faulting. Also previous knowledge of study area helps about the age of the faults so primary and secondary features are easy to understand. Gambat-Latif area is in extensional regime where we observe flower structures with negative faulting**.**

The three major normal faults were observed, F1 starting in Lower Goru and cutting upper lithology which wasn't marked here. F2 is observed at the top of B-interval till the Lower Goru where it appears to merge with F1 whereas F3 is only marked along Lower Goru cutting upper horizons. Fault orientation in the project area is NE-SW.

Defining the extension, delineation, dip direction and heave and throw of faults in the study area is known as fault correlation. It defines a network of fault from where it passes through different formations**.**

3.2.3. Synthetic seismogram Generation

Synthetic seismogram is used for well to seismic tie for reliable verification of horizons. It is a seismic response of well data. Synthetic seismogram correlates the events identified from log data in depth unit to the reflections on seismic section measured in time. The basic process for synthetic seismogram generation involves convolution a wavelet derived from seismic data with reflection coefficient (RC) derived from acoustic and density logs. Figure 3.2 contains all components essentials for the generation of synthetic seismogram for well Tajjal-03.

3.2.3.1.Synthetic matching

After developing synthetic seismogram, it is matched with original seismic section. SynView is used for synthetic editing in Kingdom software. For correct synthetic matching, a seismic trace is extracted nearest to well from seismic section. The synthetic trace is shifted, stretched or squeezed to get best matching results with synthetic seismogram. This process is repeated till synthetic trace trend starts to justify the log trends of GR, sonic, density and velocity logs along with the well tops.

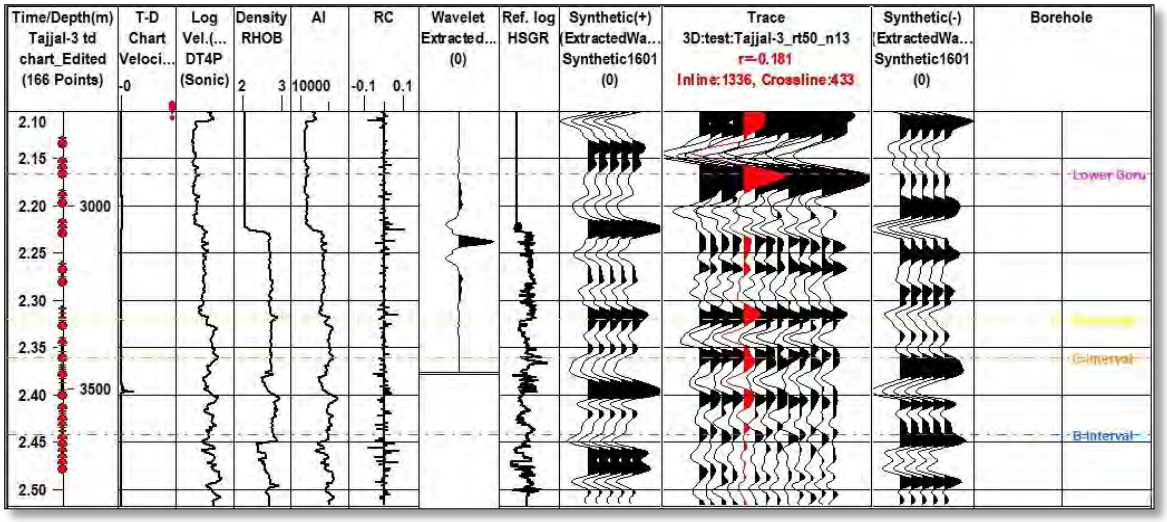

Figure 3.2. Extraction of reflection coefficient and synthetic amplitude from well logs of Tajjal -03.

3.2.4. Horizon Interpretation

The first and basic step of seismic interpretation is to interpret and mark different horizon on seismic data. To interpret correctly, one should have the knowledge about the structure as well as stratigraphy of the study area. For near to precise interpretation, outcrop data or near well tops data is correlated with seismic to precisely mark the location of horizons on seismic data.

The next step is to select the reflectors that show good character, continuity and sharp acoustic impedance contrast that can be followed throughout the area. Continuity is good where there is a sharp velocity-density contrast, thus representing a compact lithology.

In this project, four horizons have been marked. Firstly, all the horizons were marked on the control line i.e. 1338 and then the interpretation was extrapolated to the rest of the seismic lines. Horizons identified on the basis of well tops, from shallow to deep are as follows:

(a) Top near Lower Goru (Pink Horizon)

(b) Top near D-Sand Interval (Yellow Horizon)

(c) Top near C-Sand Interval (Orange Horizon)

(d) Top near B-Sand Interval (Blue Horizon)

As A-Sand Interval was penetrated neither by Tajjal-02 nor by Tajjal-03, and unfortunately the T-X Chart for Tajjal South-01 was not provided therefore it was not identified.

3.2.4.1.Seismic Section Interpretation of Study Area

Depending on the synthetic seismogram of Tajjal-03 and well tops of the Tajjal South-01, Tajjal-02 and Tajjal-03, four horizons are interpreted on time seismic section. While acquisition, inlines are positioned at the dip of the structure hence picking of horizons is done on inlines. General trend of horizons are marked at the interval of 5 inlines and then using the 3D-Hunt the horizons are marked along all the inlines.

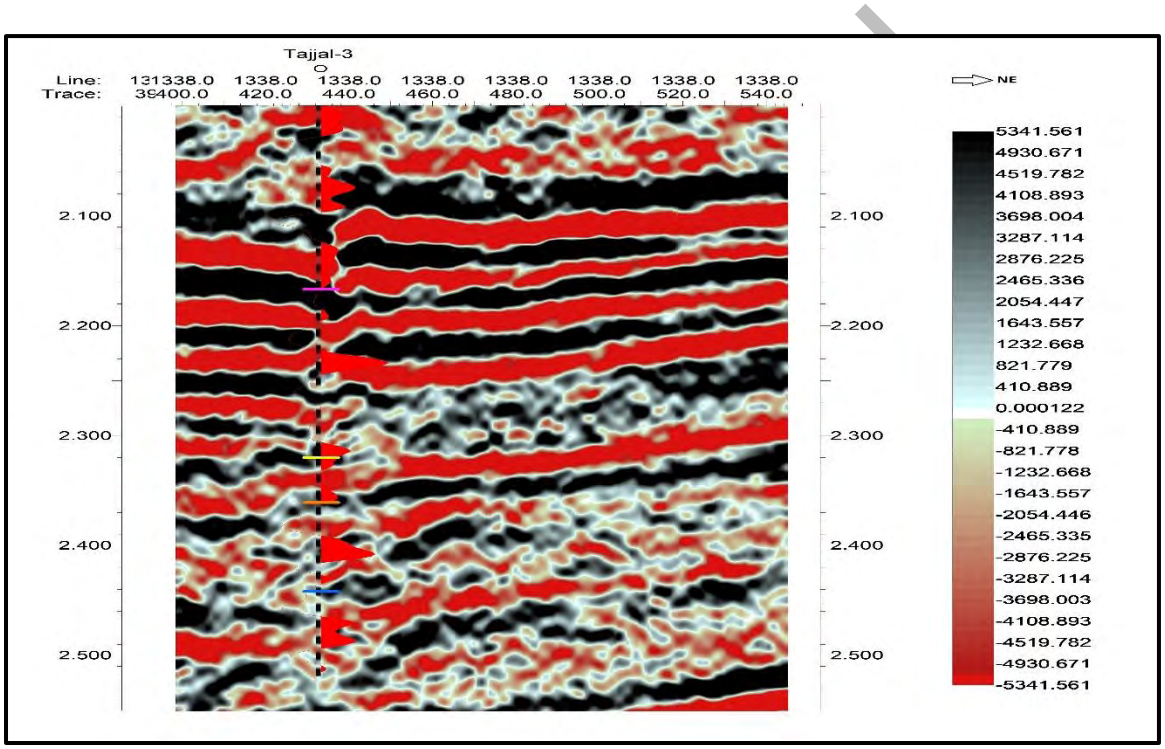

Figure 3.3. Synthetic Seismogram generated from Tajjal-03 is plotted on Inline 1338.

3.2.4.2.Conclusion of Interpreted Section

Four horizons are interpreted on the seismic sections i.e. Lower Goru Formation, D-Sand Interval, C-Sand Interval and B-Sand Interval. Horizons are dipping in the northeast direction of the study area. Seven normal faults are interpreted on seismic section i.e. . Lateral extent of F1 and F7 faults is continuous up to the last section as it covers most of the study area. Fault F1 cuts all four horizons whereas F7 is only extended up to D-Interval. Faults type indicate extensional regime that can be related to the rifting of Indian Plate in Cretaceous

Period. Figure 3.3 shows synthetic seismogram of Tajjal-03 plotted on seismic data whereas Figures 3.4 and 3.5 show interpreted horizons on inline 1338 and 1411 respectively.

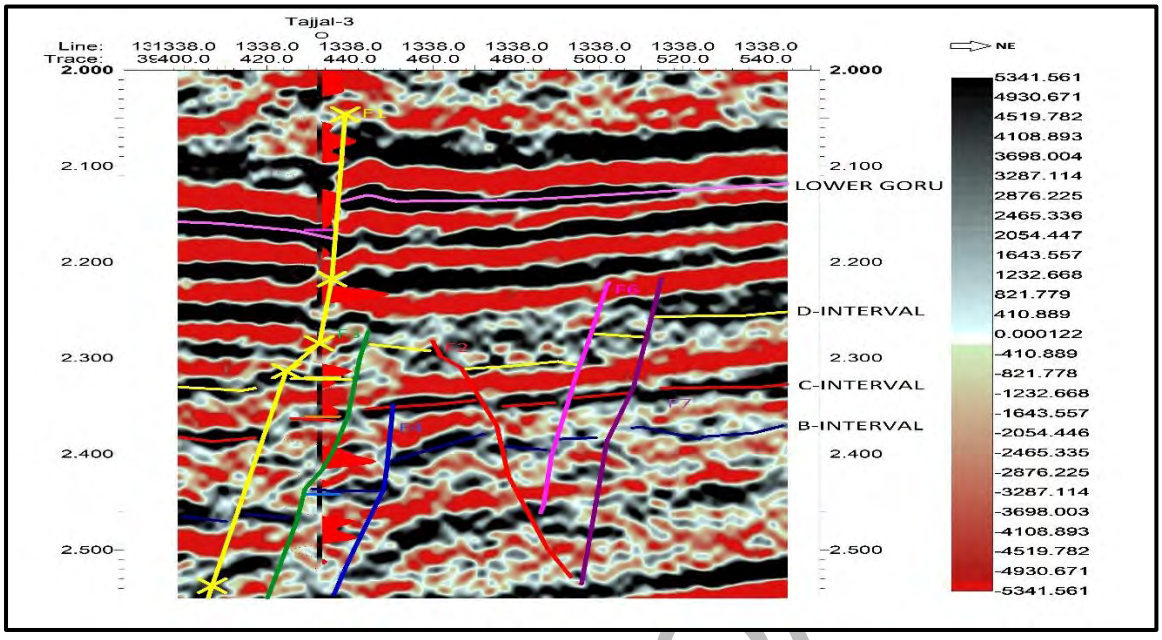

Figure 3.4. Inline 1338 is interpreted for targeted horizons using T-D chart of Tajjal-03.

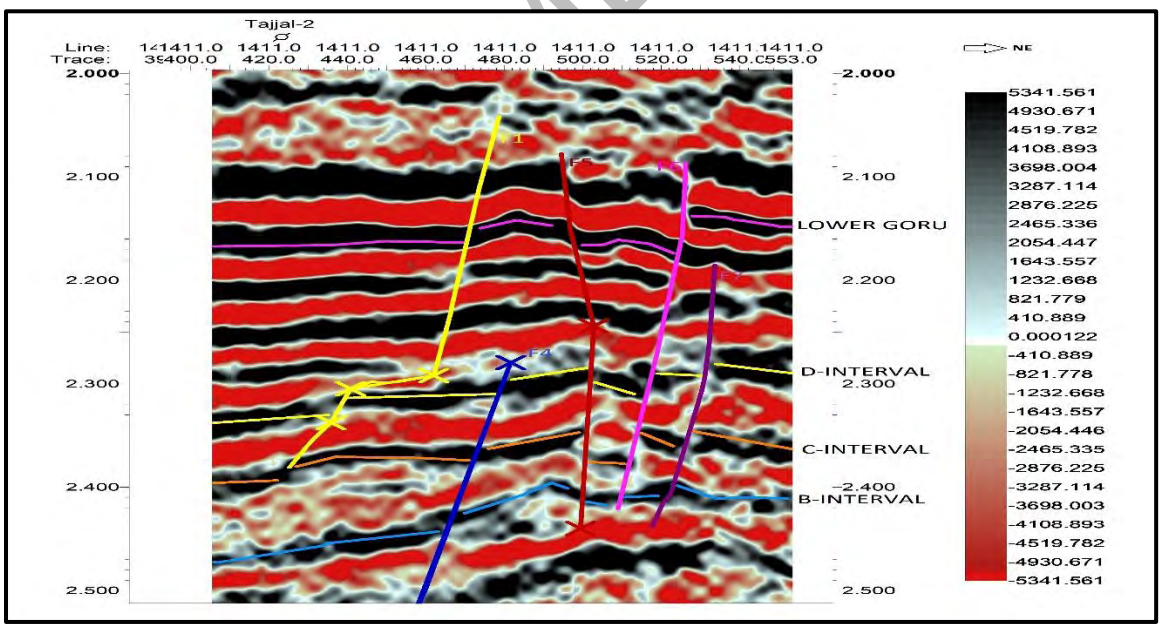

Figure 3.5. Inline 1411 interpreted for targeted horizons.

3.2.5. Construction of Fault Polygon

For construction of fault polygon, the faults are interpreted on many sections so the faults correlate with each other. The polygons can be constructed in two ways:

Manually: Manual polygons are constructed by joining the faults on the map. It describes the lateral extent of the fault by joining similar faults manually in the map view.

Auto-generated: It is done by the software itself. It also joins the lateral extent of the faults. The polygons can be visualized in cube view and map view. In our project we use auto-generated fault polygons.

3.2.5.1.Fault Correlation Displayed in Map View

Seven normal faults are interpreted on the whole 3D area, showing an extensional regime. Faults F2, F5, F6 and F7 form horst and graben structures. Lower Goru Formation and B-Sand Interval are much affected by the extension of the plates as these formations belong to Cretaceous age in which rifting of Indian plate took place. Presence of shales above and below B-Sand Interval provide seal and also act as a source for the reservoir sandstone make a complete petroleum system Faults interpreted on seismic data are shown in figure 3.6.

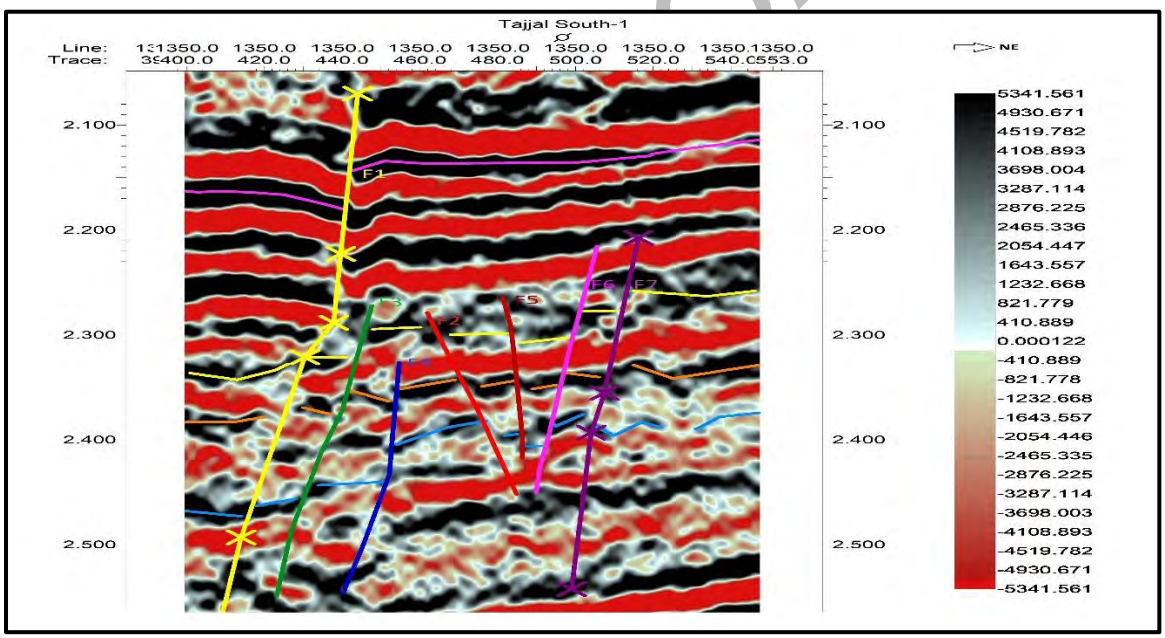

Figure 3.6. Interpreted faults displayed on inline 1350.

3.2.6. Creation of Time and Depth Structural Maps

Final stage of Interpretation is the contour map generation. Contours are lines that join the points of equal time, elevation or depth. For contour map, we generate the grid of horizon by Grid and Contour tool and then contour is generated on that grid. In seismic interpretation, first we prepare the TWT contour maps and then depth contour maps are prepared.

Contour maps; also known as seismic maps, is the final product of seismic interpretation which is essential to decisions about where, and whether, to drill well for oil (Coffeen, 1986).

3.2.6.1.Time and Depth contour maps preparation

Final step of seismic interpretation is time and depth contour maps. Time contour maps are first prepared because the data is readily available in time and then time sections is converted into depth sections with the help of velocity function to create depth contour maps. Detail of maps are given with sequence of interpretation on seismic section. Time and Depth contours for the B-Sand Interval horizons are prepared and discussed.

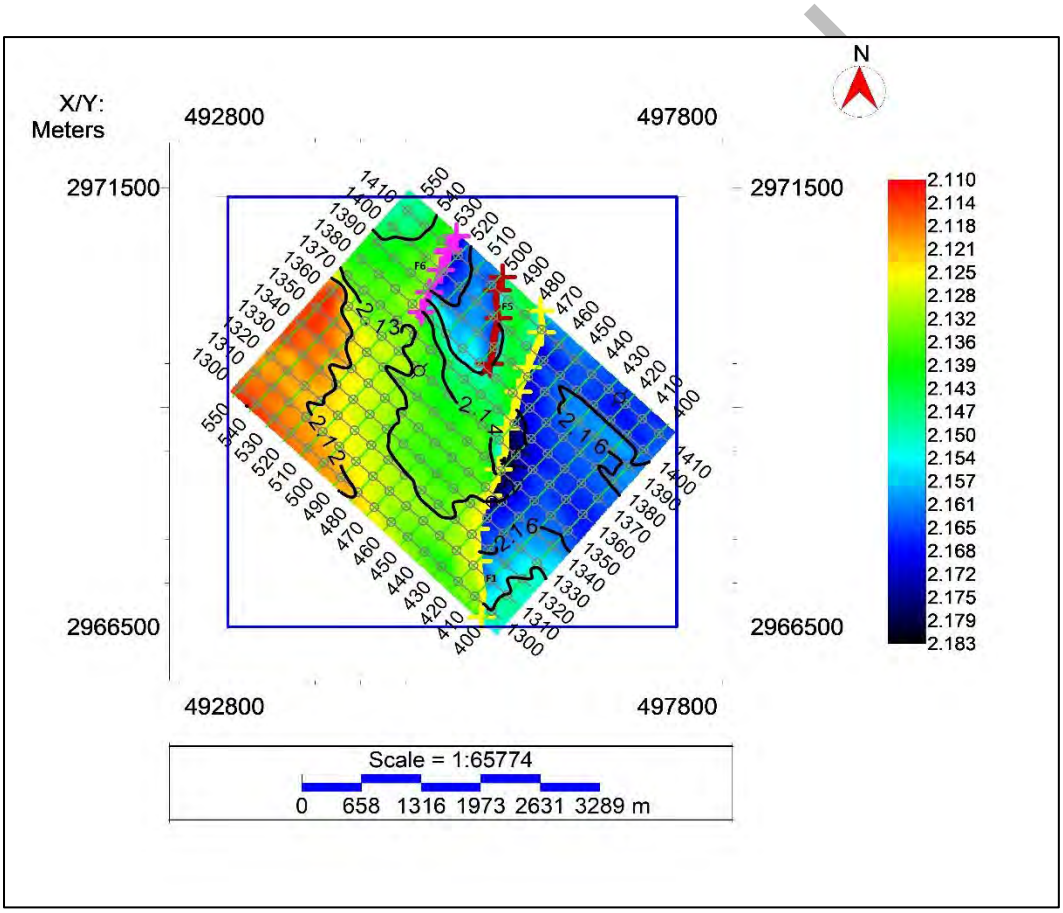

Figure 3.7. Time structural map of Lower Goru Formation showing time contours along the 3-D geometry.

Four horizons were marked on provided seismic sections that were lying in a time range of 2.1 ms to 2.6 ms. color variation in individual time grids provided an initial idea about the structural variation along the study area. The low and high time grid values show structurally shallow and deeper zones as shown in Figure 3.7, 3.8, 3.9 and 3.10 respectively. Later on time

to depth conversion was carried out using well velocities and depth values were gridded for Lower Goru and its sand units as shown in Figure 3.11, 3.12, 3.13 and 3.14 respectively.

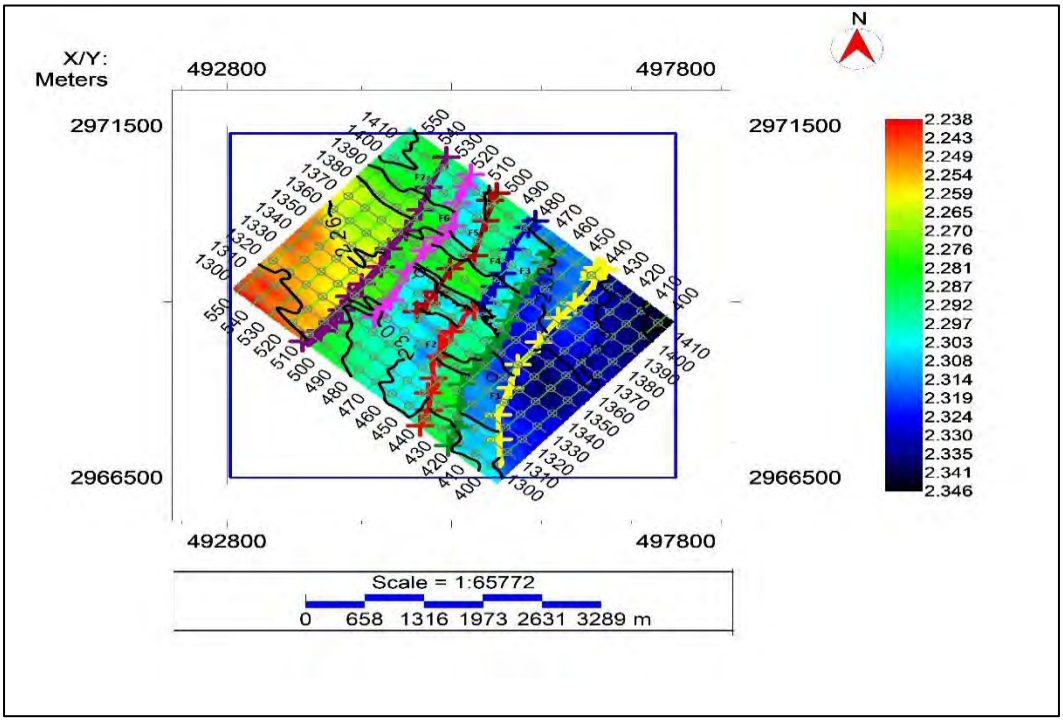

Figure 3.8. Time structural map of D-Sand Interval showing time contours along the 3-D geometry.

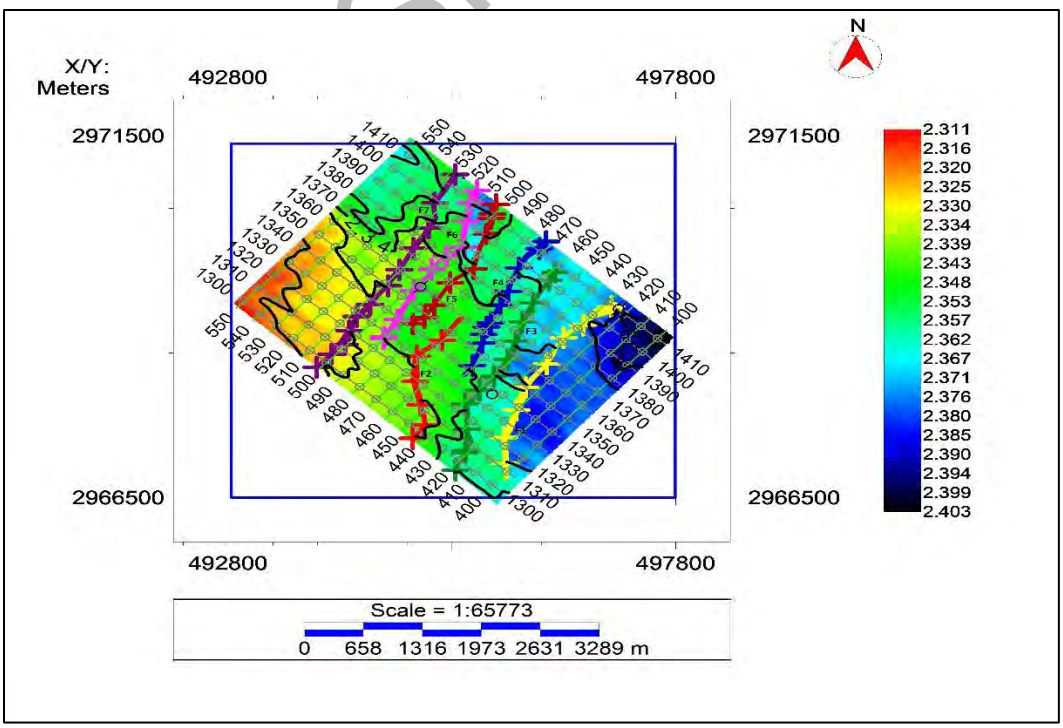

Figure 3.9. Time structural map of C-Sand Interval showing time contours along the 3-D geometry.

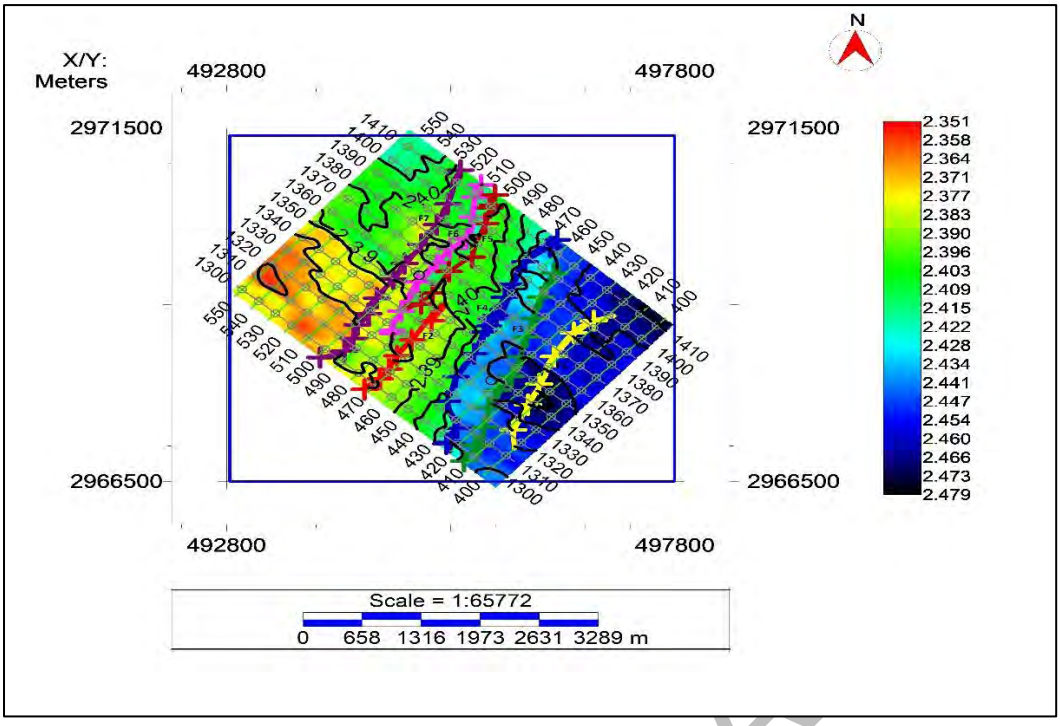

Figure 3.10. Time structural map of B-Sand Interval showing time contours along the 3-D geometry.

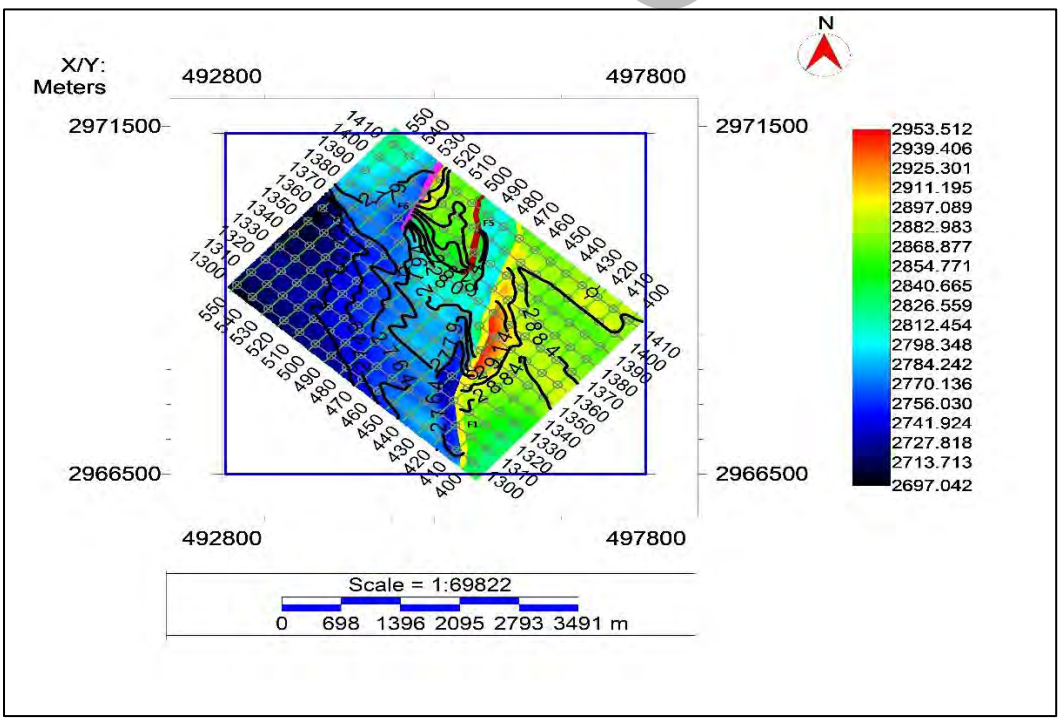

Figure 3.11. Lower Goru Formation depth structural maps showing depth contours increasing towards northeast.

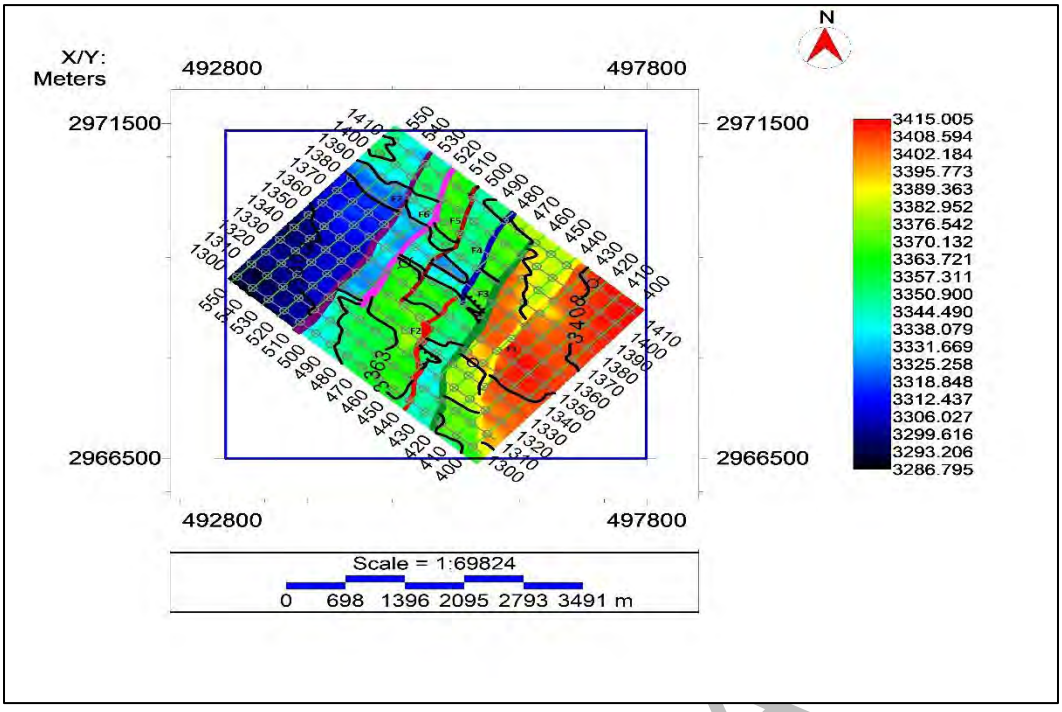

Figure 3.12. D-Sand Interval depth structural maps showing depth contours increasing towards northeast.

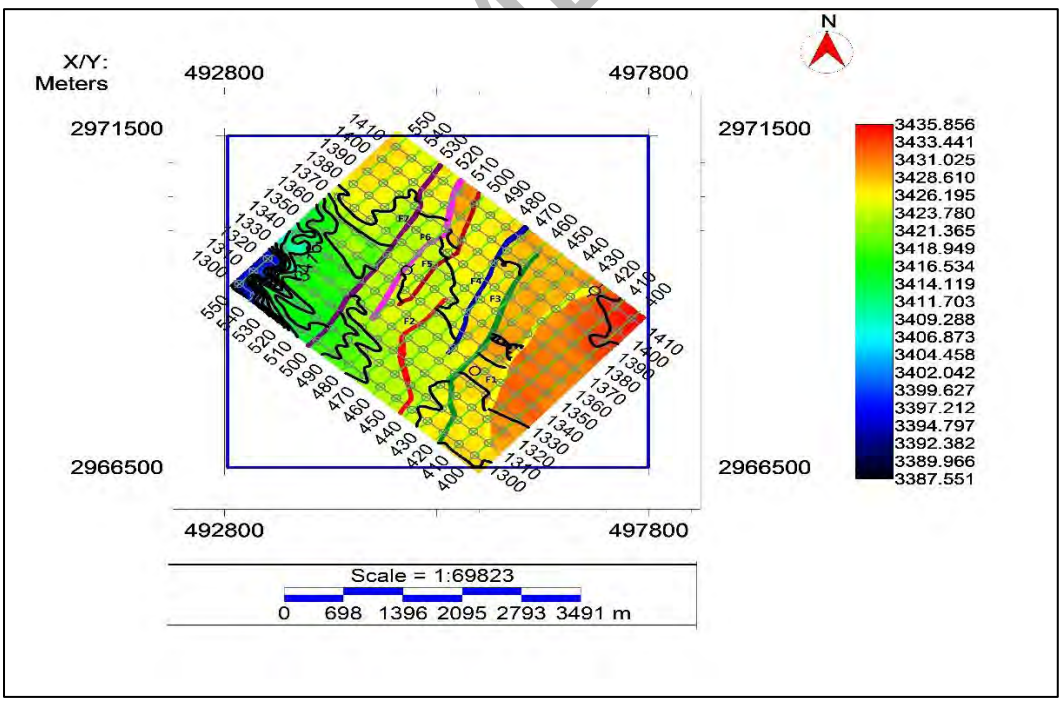

Figure 3.13. C-Sand Interval depth structural maps showing depth contours increasing towards northeast.

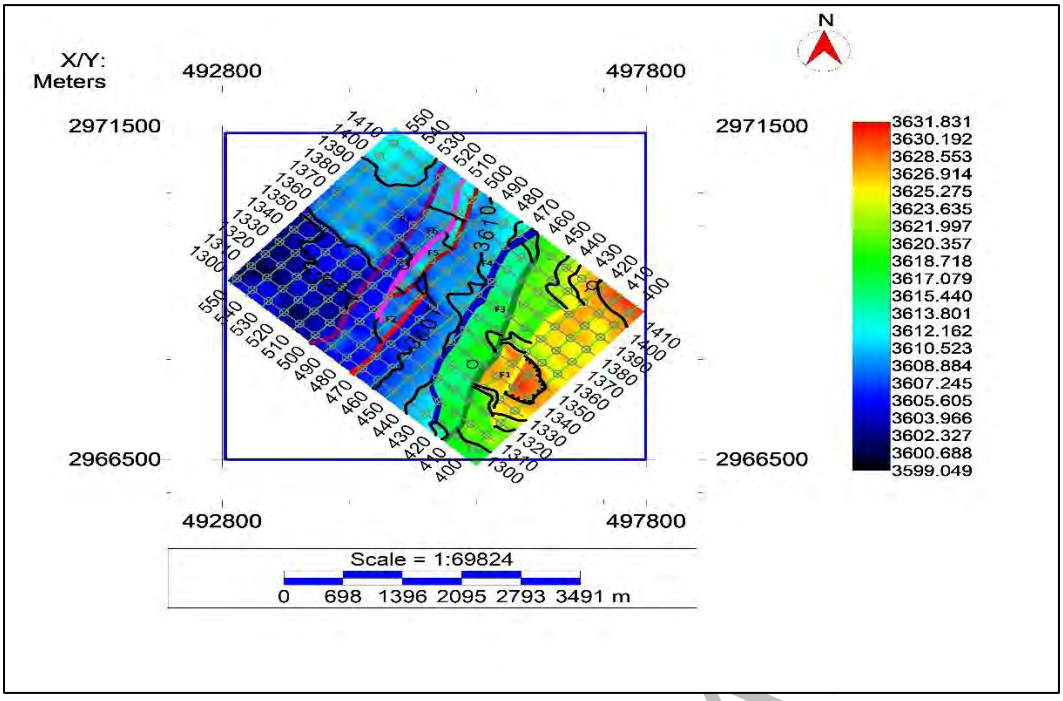

Figure 3.14. B- Sand Interval depth structural maps showing depth contours increasing towards northeast.

CHAPTER 4
SOURCE ROCK EVALUATION

4.1. INTRODUCTION

Total organic carbon content (TOC) determines the prospectivity of any shale play (Schmoker, 1989). Fine-grained sediment rocks i.e. mudstone, shale or limestone having a TOC more than 1% (by wt.) are considered to generate hydrocarbon commercially (Landais, 1997).

The traditional and relatively accurate method of calculating TOC is from core data, sidewall plugs and cuttings in laboratory. Though it is the most accurate measurement, it has its drawbacks i.e. high cost, long measurement time and non-continuous measurements and limited samples. These limitations are overcame by utilizing different continuous log data. (Alshakhs and Rezaee, 2017). Until and unless the main purpose of drilling is source rock evaluation or a source rock is above the targeted zone, log data is also not readily available for source rocks due to high costs of drilling.

Source rocks are evaluated through petrophysics using different wireline logs. Organic rich source rocks can be categorized by Gamma Ray (Beers, 1945), quality of organic matter is estimated using density log (Schmoker et al., 1989), sonic log and GR log can be used to display direct relationship with organic richness (Dellenbach et al., 1983) and combination of these logs can be used to distinguish between source and non-source rocks (Meyer, 1984).

For TOC calculation, Passey et al., (1990) introduced a new technique ΔlogR which involves the overlapping of porosity logs (sonic, neutron, and density) and resistivity logs. Different logs are observed together to mark the zones containing organic matter i.e. high hydrogen and carbon content, high resistivity, low density, higher uranium concentration and low sonic velocity values.(Herron et al., 1988).

In conventional petroleum system, sandstone and carbonates are considered reservoir rocks whereas shales and lime-mudstone containing suitable TOC are treated as source rocks. Due to their properties i.e. high GR, low density, high resistivity, lower velocity, good porosity but low permeability, shales are considered good source rock. Shale rock is generally organic

rich mudstone with 30% clay mineral, favorable amount of quartz with small quantities of feldspar, iron oxide and carbonate (Blyth and Freitas, 1987).

Unconventional resources incorporate thick crudes/bitumen, oil sands, crude oil/gas shale, tight sand gas, coal mine methane (Caineng et al; 2010). Shale reservoirs contains two different kinds of natural gas depending on the amount of Total Organic Content (TOC) present in the rock i.e. absorbed and free gas (Holmes et al., 2011). Absorbed gas is soaked up into the particles of organic matter while free gas is present within the fractures and pores of the rocks.

To examine the hydrocarbon potential of Lower Goru shale wireline log data of Tajjal South-01, Tajjal -02 and Tajjal-03 wells are used.

4.2 KEROGEN TYPE

Kerogen is a small portion of sedimentary organic components in sedimentary rocks that is insoluble in the normal organic solvents (Durand, 1980). Bitumen is considered as soluble-solvent. On heating the rock; kerogen converts into crude oil and natural gas. Source rocks are the rocks having a relatively high concentration of mature kerogen. Kerogen is classified into four types based on O, H and C ratios and origin.

4.3. WELL LOG RESPONSE IN SHALE GAS

As the source rock becomes thermally mature, a certain amount of organic material converts to gaseous or liquid hydrocarbon which moves upward and fills the pore spaces of reservoir rock by replacing formation water (Passey et al., 1990). Hence log response is very distinct in source rock as compared to reservoir rocks. Short discussion of each log in source rock is described below.

4.3.1. Gamma Ray log

Gamma ray log records the amount of gamma radiations emitted by formation. High gamma-ray intervals are associated with facies rich in organic matter. These zones are generally associated with uranium richness which is absorbed by organic content existing in marine sediments (Rider, 2002). This has resulted in increase in use of spectral gamma ray tool which provides details about heavy minerals (Swanson, 1960). Source rocks can be moderately radioactive due to high concentrations of radioactive minerals i.e. uranium, thorium and potassium, which results high GR log values in the organic rich intervals.

4.3.2. Sonic Log

Sonic log measures the acoustic transit time of the rock. Velocities V_p and V_s are inversely related to transit time. Presence of organic matter in shale is generally marked with low values of V_p and V_s due to high transit time. Organic matter rise results in decrease in density of formation in well which is also marked with increase in transit time resulting in lower velocities in source rock. For better estimation of TOC, sonic log is often used in combination with the resistivity log. Depending on the distribution of organic matter in rock matrix, transit time rises by more than 140 μs/ft with typical display of 180 μs/ft (Rider, 1986).

4.3.3. Neutron log

Organic matter is generally marked with decrease in density which results in high values i.e. higher hydrogen content recorded by neutron log in shale intervals. During the organic rich interval, higher neutron log response is associated with higher porosity values. Neutron log is not a reliable TOC estimator on its own hence it is always used in combination with density log though it is not relevant in the presence of clay formations. It is estimated that the "neutron" response to organic matter is 67(average) p.u. and that the response of the matrix is typically near zero (Rider, 2002).

4.3.4. Density log

Density log is the measure of bulk density of formation. This log typically reads low values in organic matter rich shale interval. Clay minerals are marked with average value of 2.7 g/cc on density log hence, low density values in shale interval are associated with organic richness. In combination with resistivity logs, density log is a good indicator for organic rich source intervals (Schmoker, 1979).

4.3.5. Resistivity log

Resistivity log is effected by different factors associated with organic rich shale rock. As source rocks are usually laminated so they are anisotropic in nature, which results in higher resistivity values measured by LLD. Upon the maturation of source rock, voids and fracture are filled with free oil in them. The TOC content is electrically non- conductive therefore, higher organic matter also increases resistivity of the formation (Rider, 2002). Resistivity log also acts as a maturity indicator for kerogen because resistivity is directly associated with

maturation of source rock with an upsurge by a factor of 10 or more. Resistivity log is generally used alongside porosity logs for assessment of source rock (Passey et al., 1990).

4.4. TOC CALCULATION FROM WIRELINE LOGGING

TOC is major factor in the evaluation of kerogen-rich unconventional reservoirs; hence an accurate wireline TOC log is required. Petrophysical properties of the hosting source rock matrix are highly variable with those of the organic matter present. TOC occurrence is marked with decrease in density log values along with increase in values of GR, neutron and resistivity logs. TOC of area can be predicted by using different approaches such as Schmoker, dellogR method and Meyers and Jenkyn's method.

4.4.1. Schmoker's Method

Density of organic matter is less relative to the matrix of inclosing rock. Density of organic matter ranges from 1.2 to 1.4 g/cc whereas average matrix density of shale minerals is generally 2.7 g/cc. Bulk density of any shale-rich formation is highly effected by presence of organic matter hence density log is used in most methods for calculation of TOC when other factors contributing to density variation are taken into consideration (Schmoker et al., 1979). Schmoker method (1990) relies on the principle that along with the inverse of bulk density, TOC show linear and positive correlation. Schmoker equation calculates the effects of TOC on bulk density.

$$TOC = \left(\frac{Schmoker_A}{\rho}\right) - Schmoker_B \quad (1)$$

Where, $Schmoker_A$ and $Schmoker_B$ can be computed by two methods: a) On the basis of the density of organic content along with the substance density, b) By the proportion of organic content to organic carbon. It is measured in weight percent (wt. %). Schmoker's methods divides shale formation into four components which contribute to bulk density i.e. rock matrix, pyrite, interstitial pores, and organic matter. Hence, the bulk density of the shale formation is a function of volume fractions and bulk densities of those components.

Therefore, equation can be simplify as:

$$TOC = \left(\frac{154.497}{\rho b}\right) - 57.261 \quad (2)$$

Where,

ρ_b =density log.

4.4.2. Modified Schmoker's method

TOC calculated by Modified Schmoker method is as follows:

$$K_A = \frac{1}{1-\left(\frac{1}{\rho_g}\right)} \quad (3)$$

$$K_B = K_A - 1 \quad (4)$$

$$TOC = \left(\frac{K_A}{\rho_b}\right) - K_B \quad (5)$$

Where,

ρ_g = Grain density that can either be input as a curve by the user or computed from the weight fractions.

4.4.3. DeltaLogR method

The ΔlogR by Passey 1990 is a technique where porosity logs (sonic, density and neutron logs) are overlaid on resistivity log to determine any variation in formation log response from that which is expected in absence of organic matter (Sohail et al., 2020). Presence of organic matter results in deviation in log trend of all these logs.

$$\Delta logR_{DT} = log10\left(\frac{RT}{RT_{baseline}}\right) + 0.02 * (DT - DT_{baseline}) \quad (6)$$

$$\Delta logR_{\rho} = log10\left(\frac{RT}{RT_{baseline}}\right) - 2.5 * (\rho b - \rho b_{baseline}) \quad (7)$$

$$\Delta logR_{PHI} = log10\left(\frac{RT}{RT_{baseline}}\right) + 4 * (PHI - PHI_{baseline}) \quad (8)$$

Level of Maturity is computed using laboratory Vitrinite Reflectance data.

$$LOM = (0.0989 * \%Ro^5) - (2.1587 * \%Ro^4) + (12.392 * \%Ro^3) - (29.032 * \%Ro^2) + (32.53 * \%Ro) - 3.0338 \quad (9)$$

Where,

LOM = Level of maturity

$\%R_o$ = Vitrinite reflectance value

$$TOC = (\Delta logR * 10^{2.297 - 0.1688 * LOM}) \quad (10)$$

4.4.4. Uranium method

$$TOC = (U\% * Gain) + Offset \quad (11)$$

Gain and offset to calibrate TOC from Uranium to lab measurements.

4.4.5. NMR method

NMR porosity (φ_{NMR}) when combined with density porosity can provide an estimate of the kerogen content in the formation.

$$Kerogen\ Volume = \left(\frac{\rho_g - \rho_b}{\rho_g - \rho_k}\right) - \left(\frac{\varphi_{NMR}}{HI\ Pore\ Fluid}\right) * \left(\frac{\rho_g - \rho_f}{\rho_g - \rho_k}\right) \quad (12)$$

$$TOC = Kerogen\ Volume * \left(\frac{\rho_k}{\rho_b * CONV}\right) \quad (13)$$

Where,

ρ_k = Kerogen Density

CONV = Conversion Factor

HI Pore Fluid = Hydrogen Index of Pore Fluid

ρ_g = Grain density

ρ_f = Apparent density of the pore fluid

Computed TOC using different techniques is shown in Figure 4.1, 4.2 and 4.3. TOC from Passey's method is further used. Calculations show that TOC values for wells Tajjal-02 and Tajjal-03 lies in below 6% and 3%. TOC (wt. %) values respectively shows that zones in B-Sand Interval has significant values of organic matter to act as source rock. Tajjal South-1 also shows significant values of TOC in B-Sand Interval.

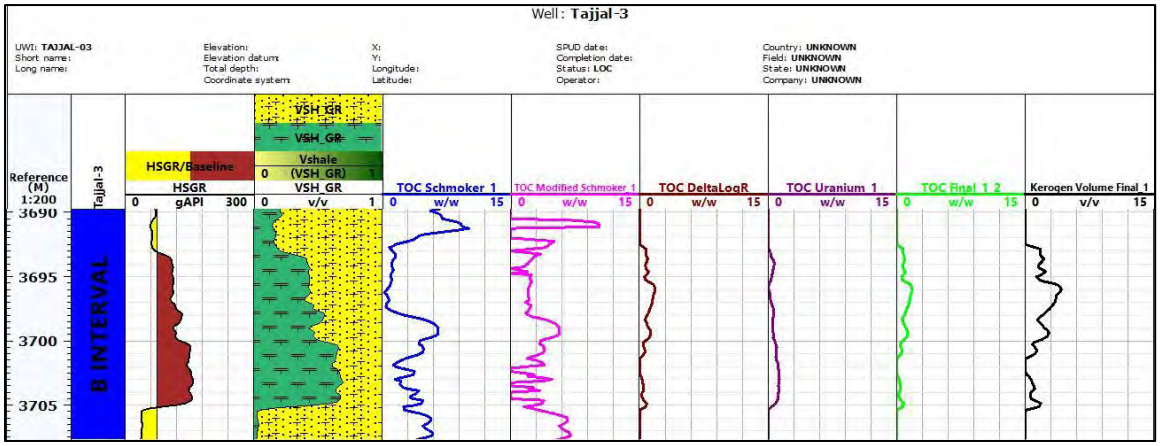

Figure 4.1. TOC calculated in Tajjal-03 zone of interest B –Sand Interval using different methods.

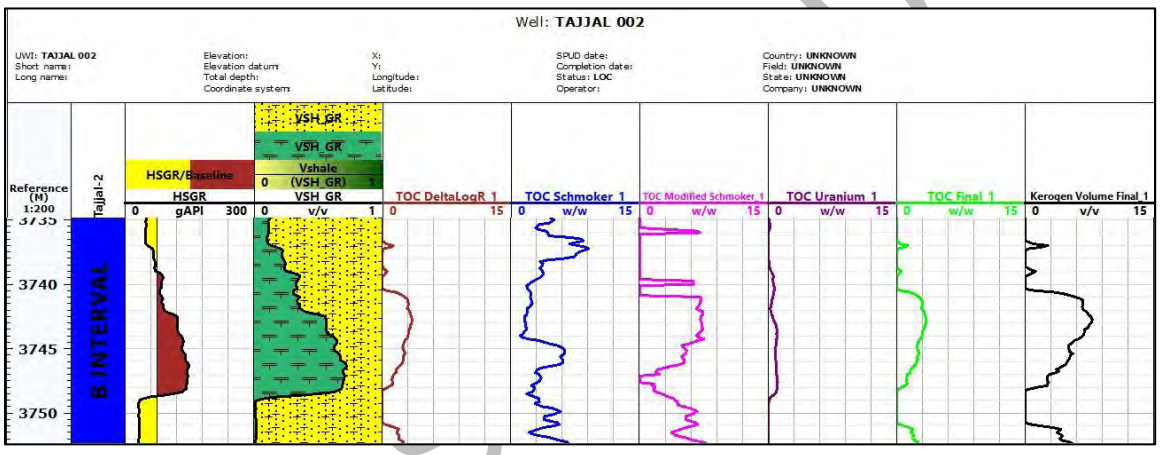

Figure 4.2. TOC calculated in Tajjal-02 zone of interest B –Sand Interval using different methods.

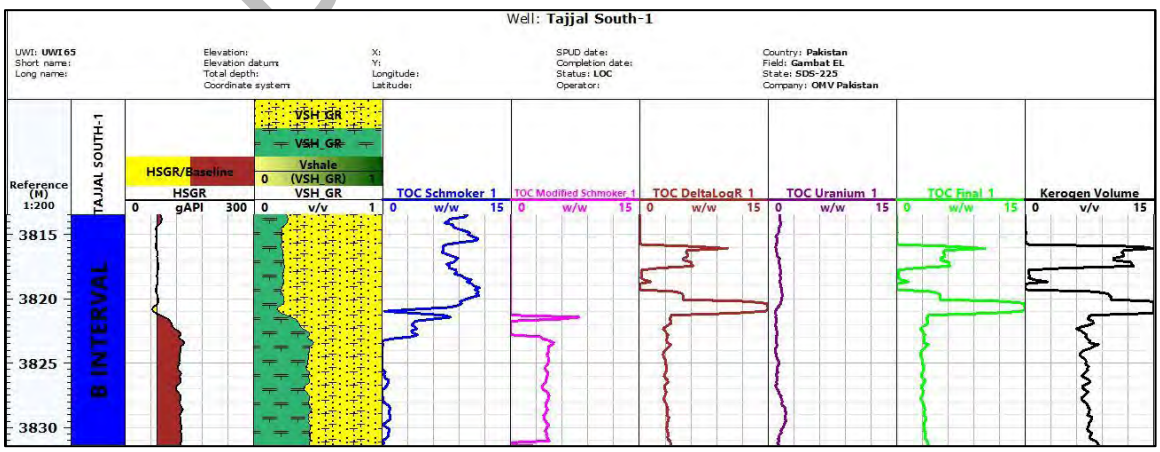

Figure 4.3: TOC calculated in Tajjal South-1 zone of interest B-Sand Interval using different methods.

4.4.6. Kerogen Volume

Herron and Tendre (1986) described a model to compute the kerogen volume from TOC.

$$Kerogen\ Volume\ = \frac{Conv*\rho_b}{\rho_k} \quad (14)$$

Where,

Conv = Conversion factor

TOC only accounts for hydrocarbons and does not provide any information for other elements within kerogen (H, O, N, and S). Conversion factor not only determines the kerogen type and maturity but also accounts for these missing elements. General value used for Conv is 1.2. ρ_k is kerogen density which converts TOC into kerogen volume. Its typical value is 1.4.

$$Kerogen\ Volume\ = \frac{TOC\ *1.2*\rho_b}{1.4} \quad (15)$$

4.5. SHALE PLAY IDENTIFICATION

In petrophysics, rock potential identification can't be done or associated with only one or two logs. It is the combination of logs which help us in identifying the potential zone. Organic-rich shale interval is generally associated with high gamma ray values (shale volume and uranium concentration), high resistivity values (maturity and anisotropy), separation between LLS and LLD logs, low density than 2.7 g/cc of shale (organic matter is less dense), high neutron log values (high hydrogen content), high transit time and low Vp and Vs values, high effective porosity, high TOC. All the qualitative and quantitative analysis led to the result that B- Sand Interval in Tajjal-03 and Tajjal-02 as shown in Figure 4.4 and 4.5 can act as prospect for source rock. Targeted zone in Tajjal-02 is 3m (3744m-3747m) which shows high GR (shale) and resistivity values (56-60 ohmm), low density (2.4-2.58 g/cc) and high neutron log values (0.6-0.13), low velocity (108-113 us/ft.) with 6-13% effective porosity and 1.2-2.5 w/w TOC values showing fair source potential in B-Sand Interval of Tajjal-02. In case Tajjal-03, targeted zone is 6m (3698m-3704m) showing high GR (shale) and resistivity values (49-69 ohmm), low density (2.34-2.6 g/cc) and high neutron log values (0.5-0.18), low velocity (104-117 us/ft.) with less than 9% effective porosity and 0.2-1.3 w/w TOC values showing very poor to poor source potential in B-Sand Interval of Tajjal-03.

Table 4.1. Classification of source potential within a formation based on TOC content. (Alexander et al., 2011)

Total Organic Carbon (%)	Source Potential
< 0.5	Very Poor
0.5 to 1	Poor
1 to 2	Fair
2 to 4	Good
4 to 10	Very Good
>10	Unknown

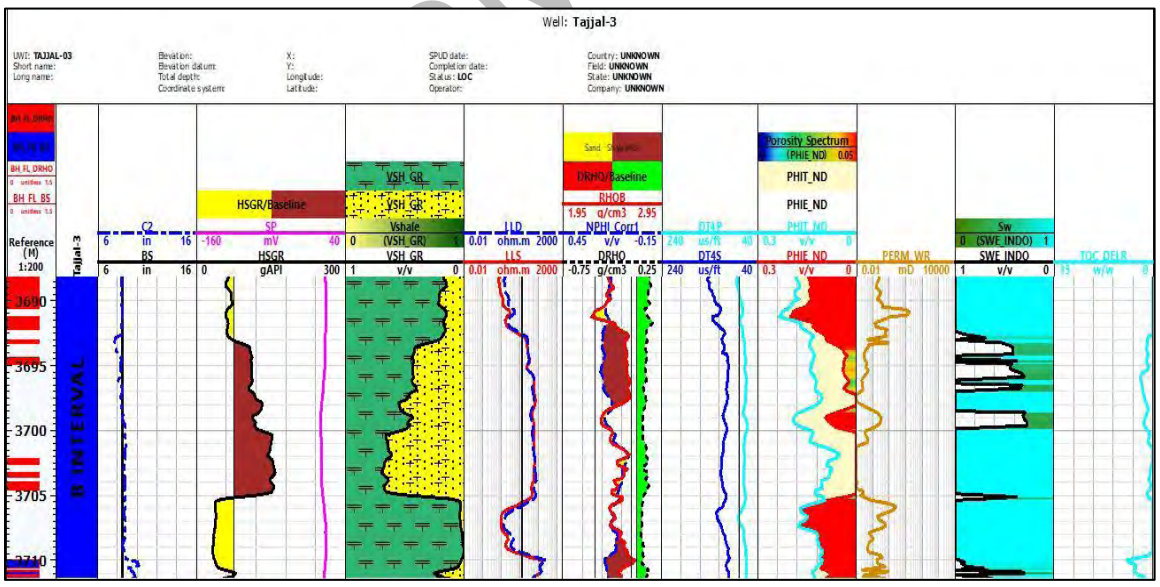

Figure 4.4. Well log responses observed in the targeted zone (3698-3704m) of B-Sand Interval of Tajjal-03.

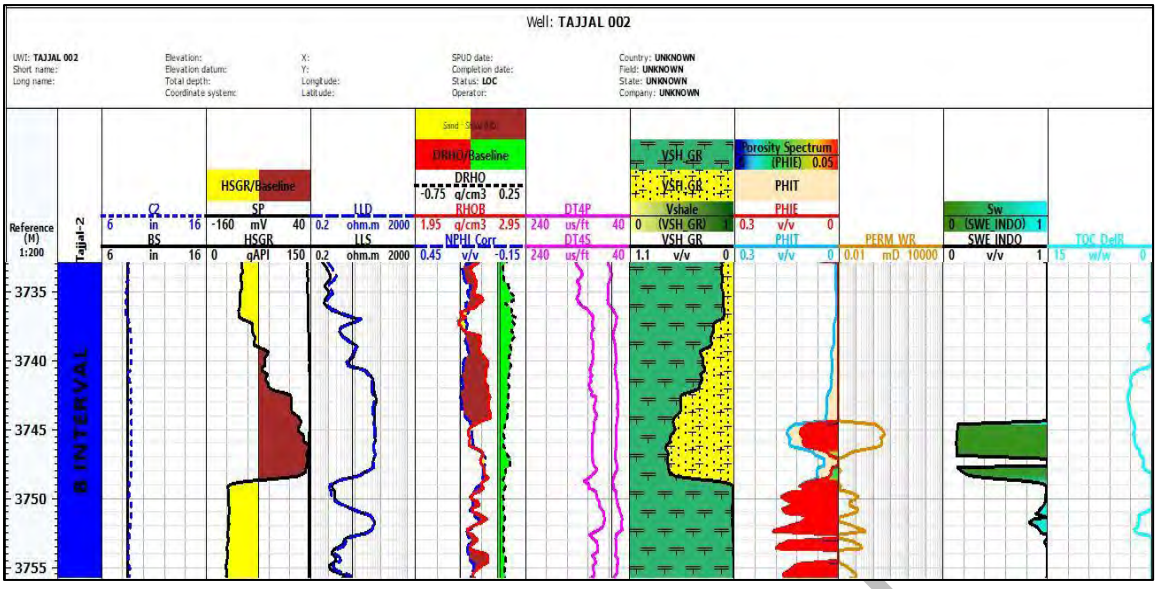

Figure 4.5. Well log responses observed in targeted zone (3744-3747m) of B-Sand Interval in Tajjal-02.

CHAPTER 5
POSTSTACK INVERSION AND TOC ESTIMATION

5.1. POST STACK SEISMIC INVERSION

Due to the efficiency and improved consistency of inversion method, exploration and petroleum industries are dependent on it to better interpret seismic data and extract physics properties of rock and fluids in targeted strata. It gives a clear image of subsurface geology. Inversion alters seismic to the blocky response that corresponds to acoustic impedance and helps define geological boundaries and recognize sweet spots (Barclay et al., 2007). Seismic data provide rich knowledge on the reservoir's lithology and physical characteristics. Seismic inversion transforms the property of interfaces into a stratigraphic property, which can be directly linked to the log information. In this way, the geological analysis made from seismic data and inverted data is useful for characterizing the reservoir. It is a well-known method since 1977(Pendrel, 2001).

Inversion is the mechanism by which seismic data is transformed into seismic acoustic impedance (AI), a product of velocity and density difference in sub-surface. Impedance is a rock property that can be related to layers (Vecken, 2004). The impedance inverted model is used by seismic analysts to estimate seismic velocities, elastic properties, density etc., all of which are helpful in understanding fluid characteristics. Impedance varies with porosity, lithology, depth, fluid content, temperature, and pressure so it can be used as a quantitative porosity and hydrocarbon measurement. Results of inversion affect the interpretation and are helpful in decision making in the exploration industry (Vecken, 2004).

Inversion or inverse modelling refers to obtain the relative acoustic impedance section using inverse of the extracted wavelet and its convolution with the reflection coefficient series. The wavelet should be extracted from the well location on seismic data. It is an iterative process and involves the improvement of extracted wavelet multiple times until we get a best match and the results are near to our ideal model. Building a geological model is the first step of inversion technique followed by matching it with the original seismic data. Model parameters are changed until the data computed is interrelated with the seismic data observed (Barclay et al., 2007). Finally, the matched geological model helps predict the distribution of the physical properties of the reservoir (Vecken, 2004).

For this purpose, various post-stack inversion algorithms are available:

1. Colored Inversion
2. Model Based Inversion
3. Band Limited Inversion
4. Sparse Spike Inversion

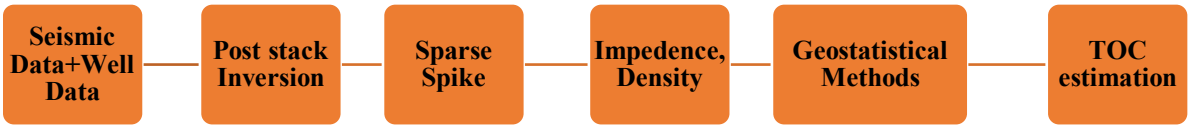

Figure 5.1. Flow chart of inversion method

For pre-stack seismic data, fluid and lithological properties are estimated by AVO analysis i.e. amplitude variations with offset whereas during post-stack inversion (at zero offset), amplitude is converted into a volume of acoustic impedance using geological, seismic data and well logs. Seismic showing amplitude is converted into acoustic impedance contrast volume in post-stack inversion (at zero offsets) using seismic, geological data and well logs. Figure 5.1 shows the methodology followed during post-stack inversion.

The primary data for the post stack inversion process is seismic, well data, and horizons. Well data of wells, Tajjal South-01, Tajjal-02, and Tajjal-03 are available. The current study is done on post stack 3D seismic data of Gambat-Latif Field.

5.1.1. Sparse Spike Inversion

Sparse spike inversion is dependent on the model and is based on the assumption that the reflectivity is composed of a series of large spikes merged on the background of small spikes until a good correlation is reached between the synthetic seismogram and the seismic trace. The inversion method simulates a synthetic seismic trace from a simplest possible reflectivity model that matches with the input seismic trace. Two types of Sparse Spike inversion method popularly used in the seismic industry are utilized in the present study - Linear Programming sparse spike inversion (LPSSI) and Maximum Likelihood sparse spike inversion (MLSSI) (Maurya et al., (2016).

Using programming technique that utilizes frequency domain constraints to recover the higher frequencies of the seismic spectrum, an estimate of the reflectivity is extracted which is integrated under the initial model. This results in a sparse reflectivity which then produces the best match between derived synthetic and the seismic trace, subject to the constraint that the number of error be a minimum. In this method, it is assumed that wavelet in the seismic data is known. This method attempts to recover an impedance model with sparse reflectivity by minimum error between the modeled trace and the seismic trace. It results in an earth model with the number of layers (Maurya et al., (2016).

LPSSI defines relative acoustic impedance. Absolute acoustic impedance is a basic physical property of rock. In this inversion algorithm low frequencies (approximately 0-15Hz) are added as component of the inversion. A low frequency model is based on well data and it is a must to achieve absolute acoustic impedance in LPSSI (Ali et al., 2018).

5.1.1.1.Methodology adopted for seismic inversion on CGG Hampson Russel Suite (HRS)

For Seismic inversion, "STRATA" module in "Geoview" application of HRS is utilized. Post-stack seismic data merged well data giving acoustic impedance volume as an output of seismic inversion. The linear-programming sparse spike inversion is able to estimate both lithology and characteristics of fluid. The lateral and vertical changes of acoustic impedance for LPSS inversion provides excellent match with well data.

Seismic and well data are loaded into Geoview from where this loaded data becomes available for "STRATA" to perform inversion. The next step was to open the project in 'STRATA'. The interpreted horizons of Lower Goru Formation were imported from Kingdom software in 'STRATA' module. After importing the horizons, statistical wavelet was extracted using seismic data only. In both time and frequency and time domains extracted statistical wavelet got displayed.

Then an initial low frequency model was build. An acoustic impedance volume is generated by post stack seismic inversion. Density and sonic logs generate P- wave impedance (acoustic impedance inversion). On both sides of well generated synthetic seismogram was extrapolated. Objective function is defined as the difference between generated synthetic seismogram and original seismic section. The difference between original seismic and synthetic seismogram became minimized by running iterations for as much times.

The next step was to apply LPSSI on seismic data and as a result an inverted seismic section was generated. In the form of acoustic impedance contrast it gives information that assist to interpret changes in subsurface geology i.e. lithology etc. and to develop its link with source rock characteristics.

In 'STRATA' module of CGG Hampson Russel suite after developing a statistical wavelet. Seismic curve data was inserted (inserted curve data: P-wave). Horizons which are interpreted also showed over it.

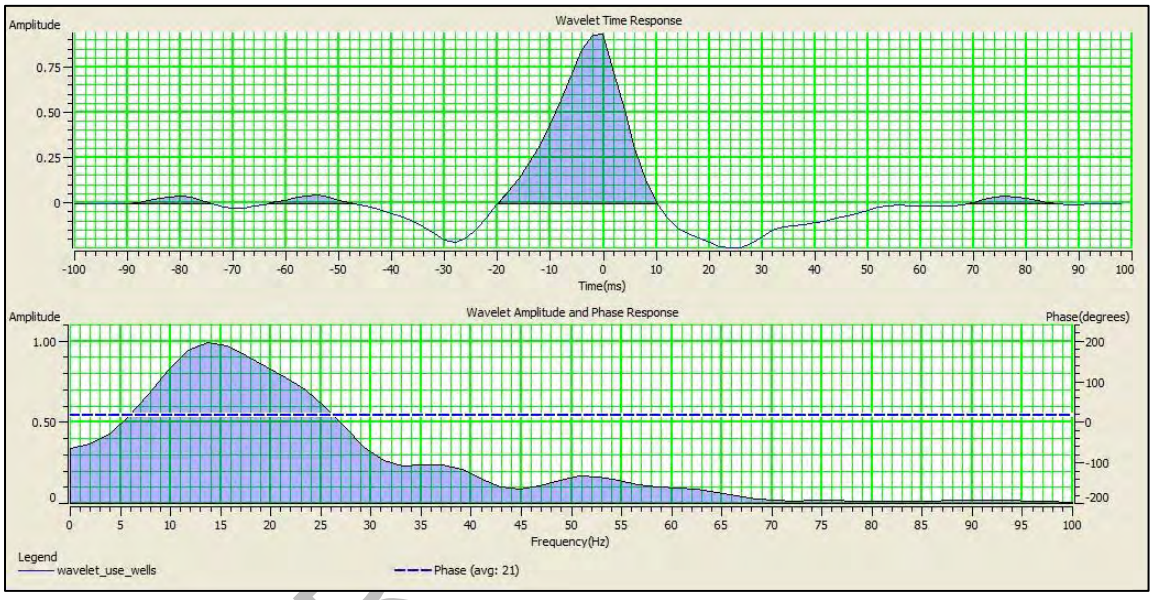

Figure 5.2. Statistical wavelet extracted using seismic data input from all wells in both time and frequency domain.

Seismic inversion is determined by the convolution model which depends on synthetic trace St (). Earth's reflectivity series is convoluted with a desired wavelet to develop the seismic trace.

$$S\,(t)\;=\;W\,(t)\;*\;R\;+N \tag{16}$$

Where,

W (t) = extracted statistical wavelet

R = reflection coefficient (RC) series

N =random noise.

Extracted and inverted reflectivity from seismic data at all wells are correlated using an estimated a constant phase wavelet (Ali et al., 2018). For the wavelet extraction, a window length of 2000 ms to 2700 ms is used in which zone of interest lies. The wavelet is kept either minimum or zero phase as shown in Figure 5.2 to acquire perfect results from seismic interpretation and inversion. Inversion results are highly effected by the extent of phase shift in input wavelet. Depending on the size of the phase shift, the error percentage in the resulting impedance data will increase (Ali et al., 2018).

In next step seismic and well data is correlated with the synthetic trace shown in Figure5.3. By using extracted wavelet, synthetic trace is generated. Correlation allows well and seismic tie. It is very important in seismic interpretation.

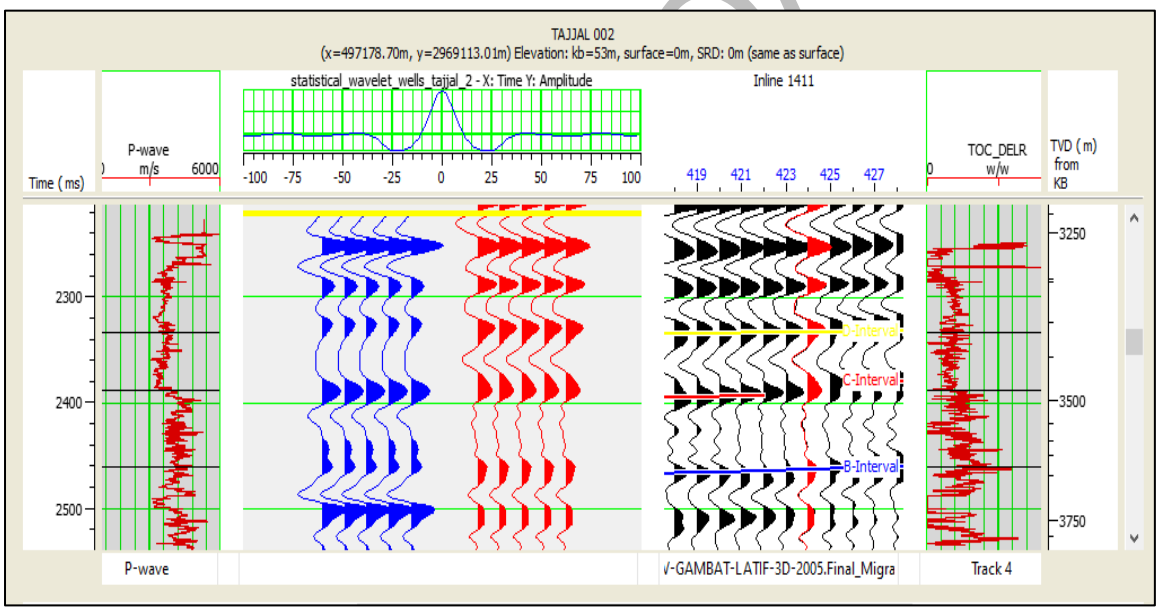

Figure 5.3. Correlation of seismic and well data with synthetic trace.

The next step was to generate low frequency initial impedance model using the impedance curve developed by well data. The initial model of seismic inlines 1338 and 1411 shows horizons within the time range of 2000ms to 2700ms where zone of interest lies. For inversion process full seismic section was used. Time in milliseconds in shown along Y-axis and X-axis represents xlines.

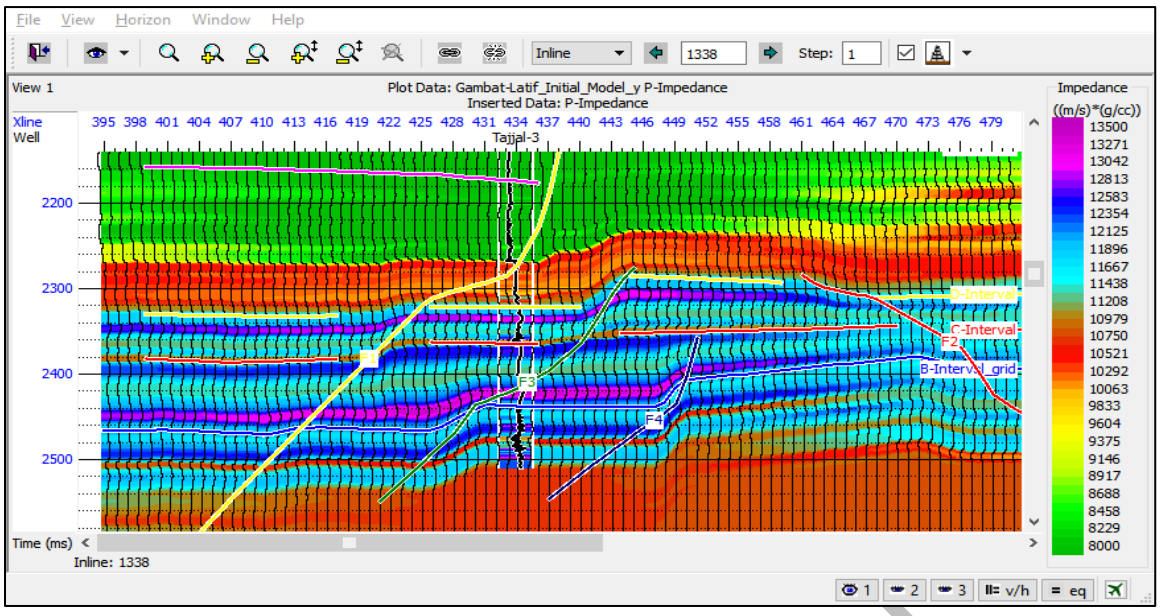

Figure 5.4. Low frequency model used for seismic inversion algorithm at inline 1338 along with impedance log generated from Tajjal-03 is displayed.

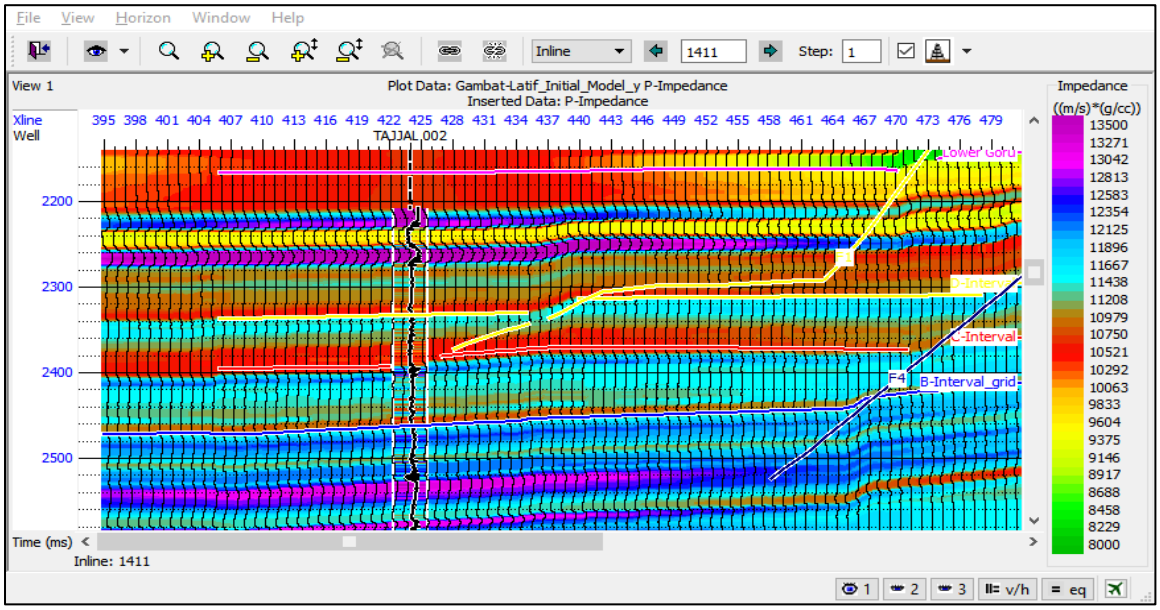

Figure 5.5. Low frequency model used for seismic inversion algorithm at inline 1411. Impedance log generated using Tajjal-2 is also displayed.

During seismic processing and stacking of data, low frequencies are lost which are recovered during inversion.

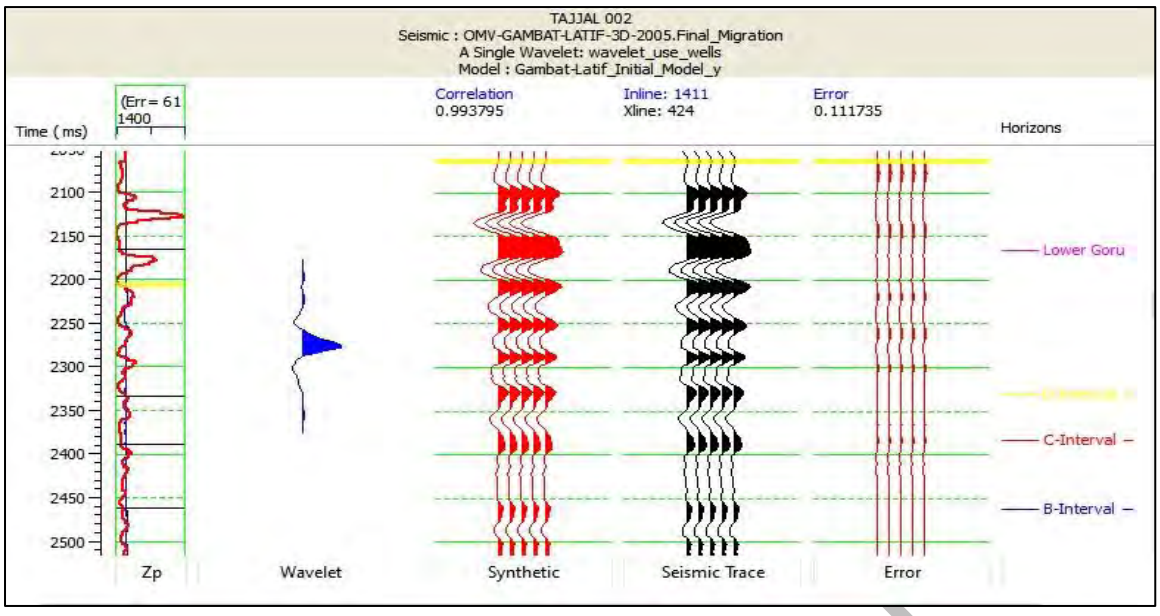

Figure 5.6. 98% correlation achieved after performing LPSSI analysis with inverted impedance (red) and original impedance (blue) at Tajjal -02.

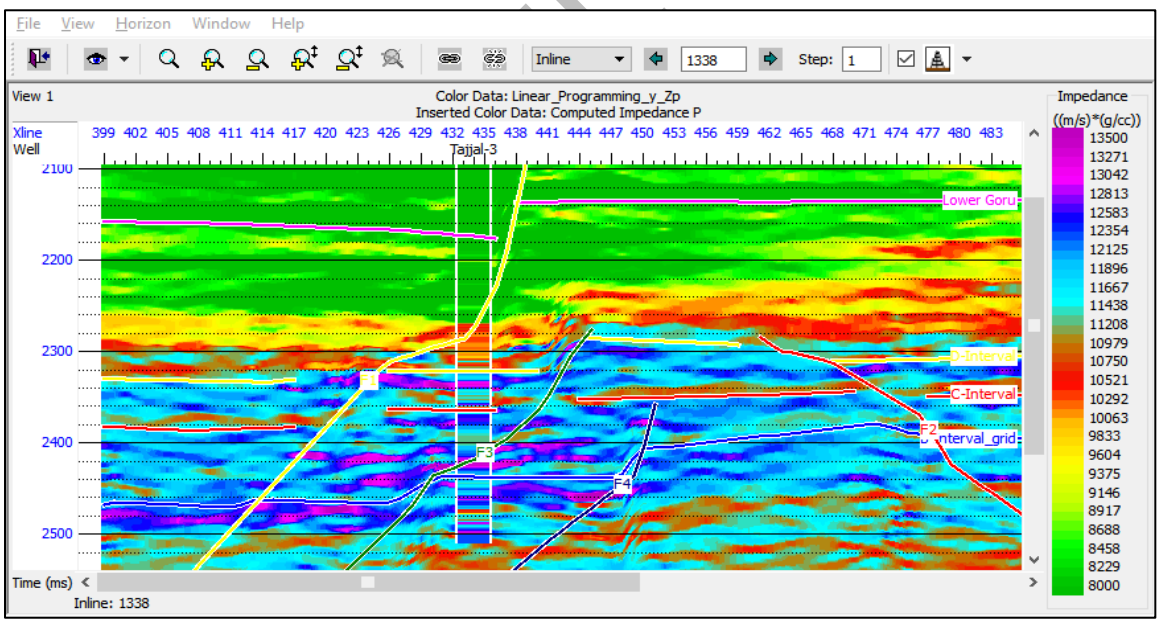

Figure 5.7. The inverted impedance of LPSSI at inline 1338.

After an initial impedance model is developed, inversion analysis for LPSSI is performed and applied at well locations for QC. Figure 5.6 shows the result of inversion analysis which gives three traces as output i.e. the synthetic traces calculated from this inversion (red), the original seismic composite trace (black) and the error trace (red) which

gives the difference between the former two traces. 25 iterations are applied on the data till we reach the desired correlation i.e. 0.993 with minimum error i.e. 0.11 as shown in Figure5.6. This high percent of correlation and practically zero error indicates that the inversion is mathematically correct, i.e., the synthetic trace created by inversion matches with the real trace.

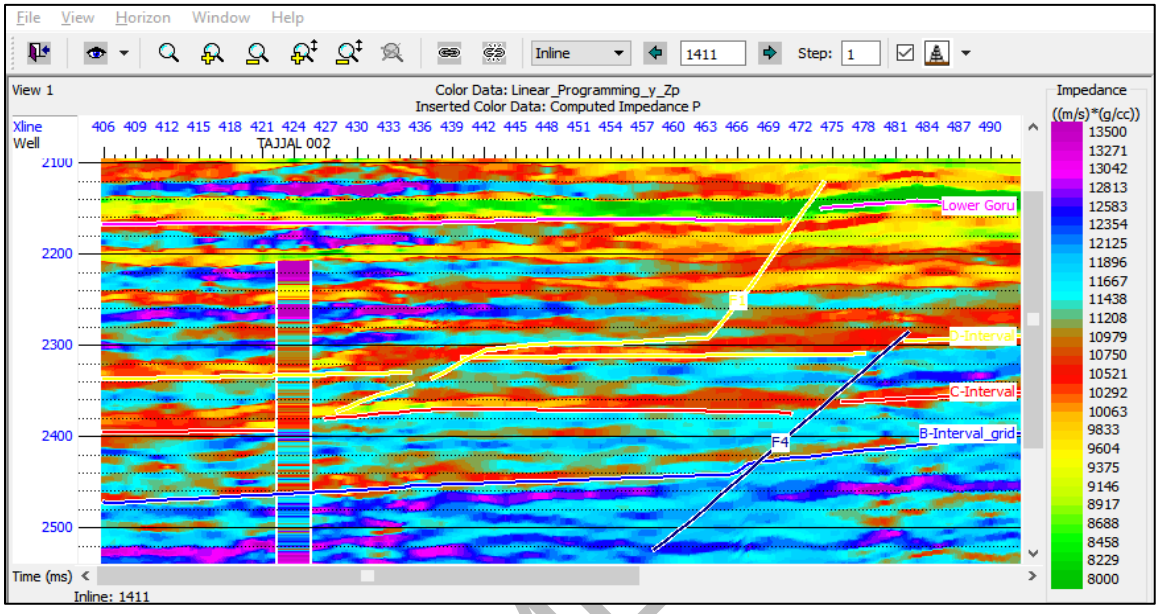

Figure 5.8. The inverted impedance of LPSSI at inline 1411.

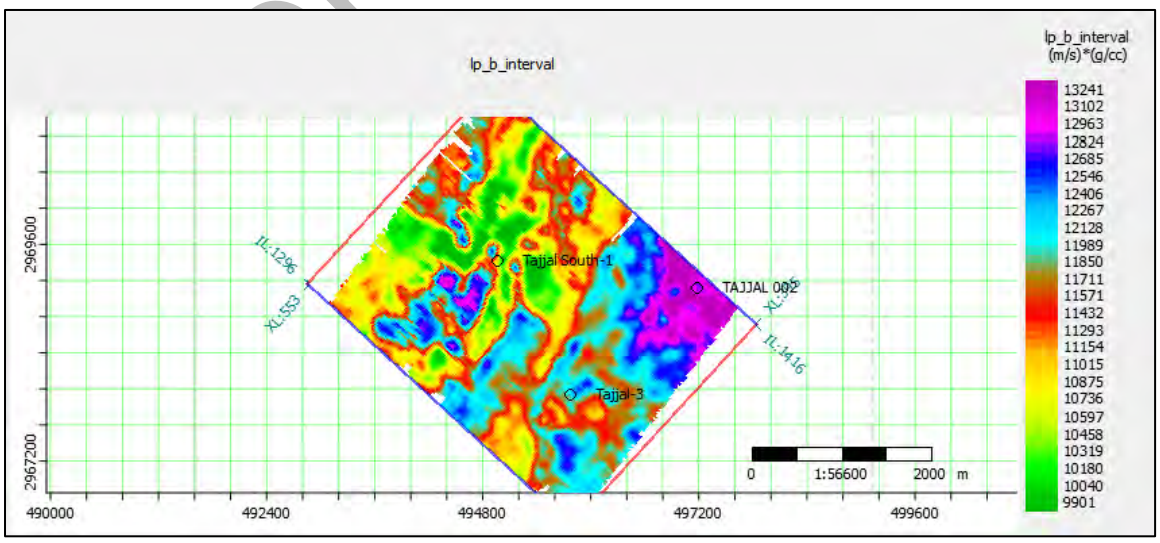

Figure 5.9. Horizon map of the top of B-Sand Interval resolved by LPSSI.

Figure 5.7 and 5.8 show the final inverted seismic data for the inline 1338 and 1411on which wells Tajjal-03 and Tajjal-02 are located respectively. Impedance log of both wells is displayed over both models to show the well and seismic impedance comparison. B-Sand Interval is the main producer of Tajjal gas field. So, final impedance model results focused at this level suggests lower impedance values in B-Sand Interval as compared to surrounding sand units.

Figure 5.9 is the data slice of B-Sand Interval showing variation in impedance across the area of study. Relatively lower impedance zone can be observed at Tajjal South-1 and Tajjal-03 well locations. Low impedance value is shown on the North West with increase in impedance values towards North East where Tajjal-2 is located.

5.2. TOTAL ORGANIC CARBON ESTIMATION

After stacking, seismic amplitudes are driven mainly by changes in the acoustic impedance contrast. TOC is associated with acoustic impedance hence also associated with seismic amplitude data (Broadhead et al., 2016). Several studies have shown that with increasing TOC there is a decrease in Bulk density and velocity (Prasad et al., 2011). In other words, acoustic impedance (AI) will also decline in accordance with TOC.

As the "P-Impedance" value increases, the TOC value declines. Thus, this relationship is used by inversion to extend impedance values into TOC by using the Hampson-Russell Emerge Predict tool. The input data requires for the computation of TOC across the survey is the "Average TOC" curve which was computed earlier using Passey's Method.

Well logs and attributes from seismic data are merged to predict a well log property volume in emerge module. These attributes from seismic data are volume attributes, such as Instantaneous Amplitude, which can be estimated from the input seismic data on a sample-by-sample basis. The predictive power and resolution of the derived TOC volume will increase due to non-linear linear characteristics of the neural network (Pico et al., 2017). In emerge process, we go through three different correlations analysis: single-attribute, multi-attribute and neural networks. One of the objectives of Emerge is to improve on this prediction using other attributes of the seismic data.

Single attribute analysis shows the target and the attribute, along with the correlation value and the statistical error associated with that target-attribute pair as shown in Figure 5.10.

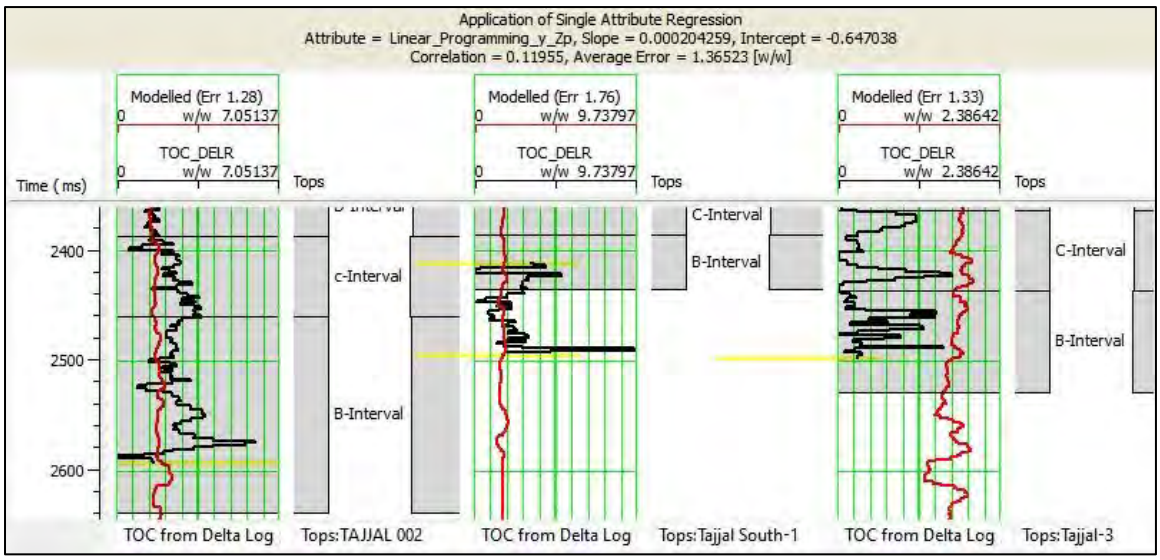

Figure 5.10. Single attribute analysis showing the target log for each well along with the "predicted" log using the selected attribute and the derived regression curve.

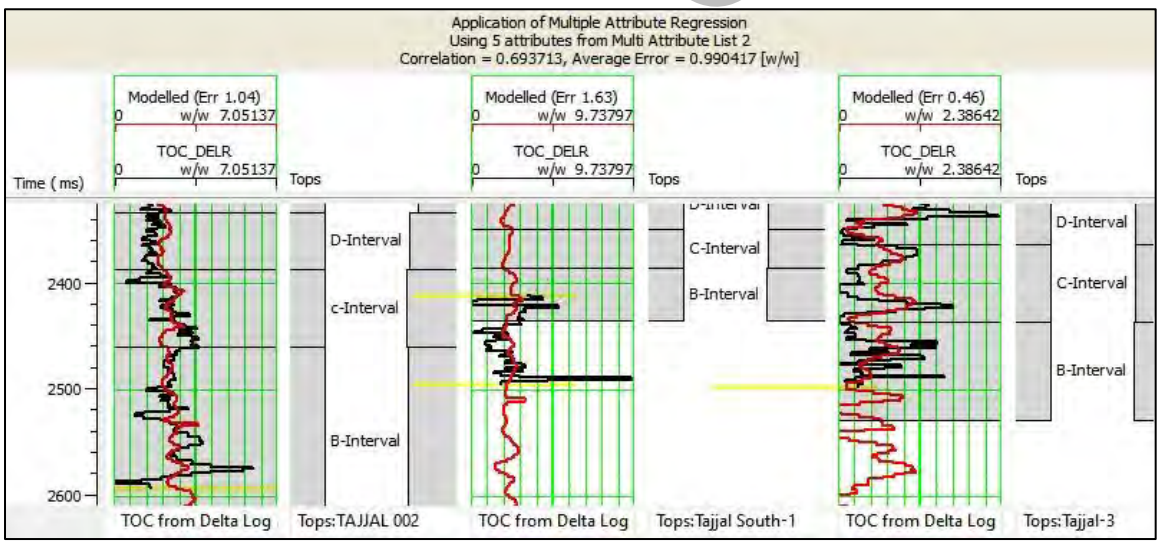

Figure 5.11. Validation of multi-attribute regression using selected attributes for each well.

Emerge uses step-wise regression to search for groups of seismic attributes which can predict the target. For this purpose, Emerge searches for such single attributes from the list that predict best by themselves (Kelishami et al., 2022). The attributes calculated are used simultaneously to improve the predictive power. The contributing features of several attributes combine to distinguish subtle features on the target logs, which cannot be predicted individually by attributes. The criterion for evaluating the prediction is the RMS error.

Mathematically, the correlation increased from 11% to 69% after comparing with single attribute analysis as shown in Figure 5.11.

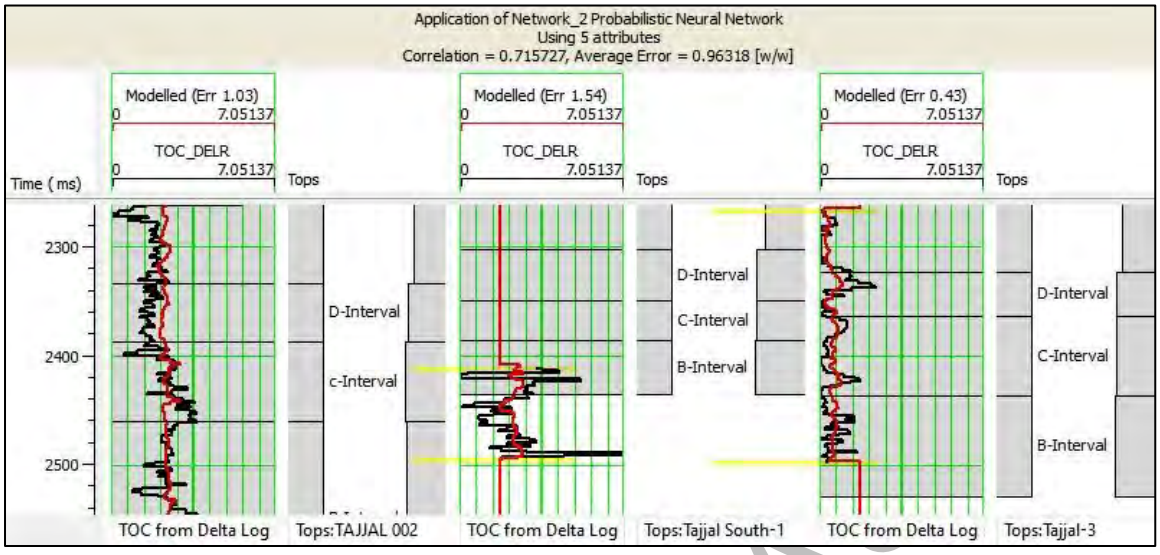

Figure 5.12. The correlation is much higher between targeted and predicted logs by neural network than that achieved with multi-attribute regression.

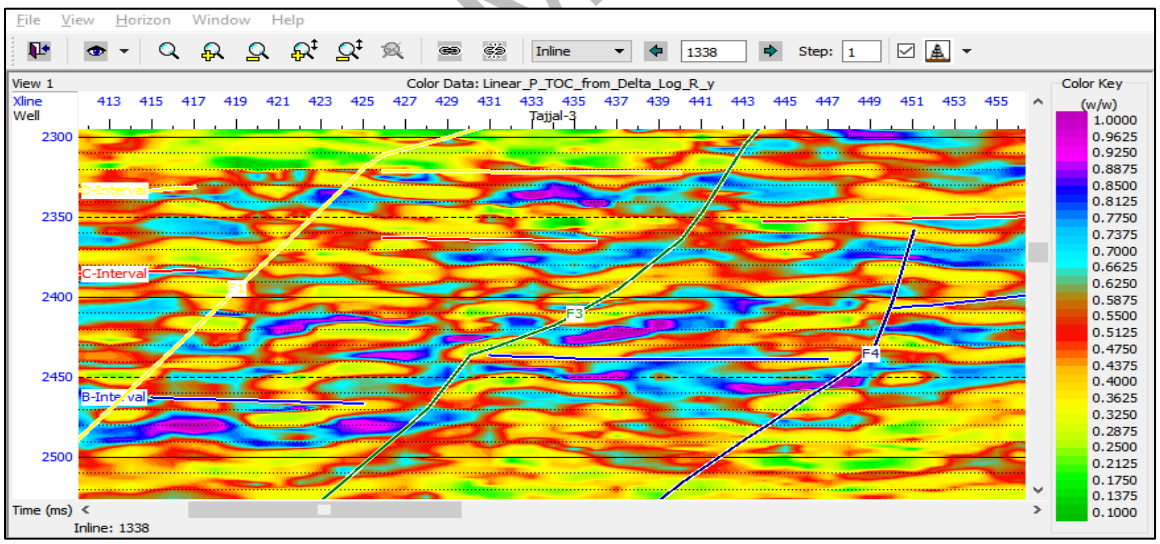

Figure 5.13. Computed TOC using neural network applied on seismic volume at Tajjal-03.

After single attribute and multi-attribute analysis, the neural network technique is further used to improve the TOC prediction. By selecting the four attribute (called Integrated Absolute Amplitude), Probabilistic Neural Network was precisely constructed with the same

attributes as those used in that multi-attributes analysis. The predictive power and resolution of the derived TOC volume will increase due to non-linear linear characteristics of the neural network. Note that the correlation of 71% is much higher than that achieved with multi-attribute regression as shown in Figure 5.12.

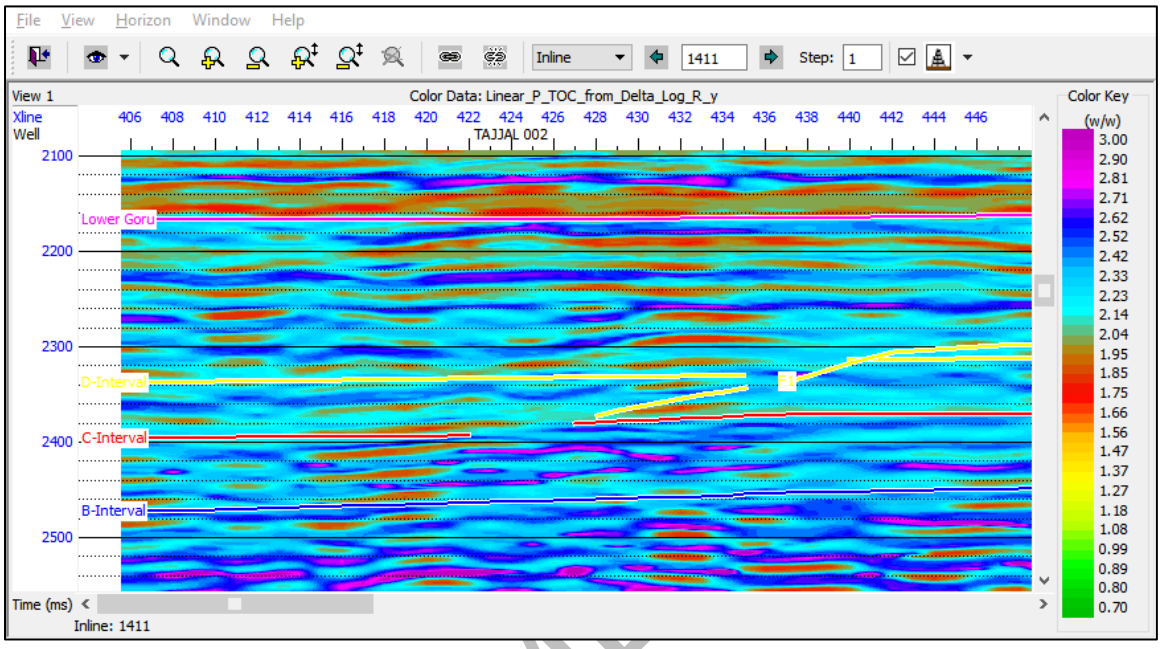

Figure 5.14. Computed TOC using neural network applied on seismic volume at Tjjal-02.

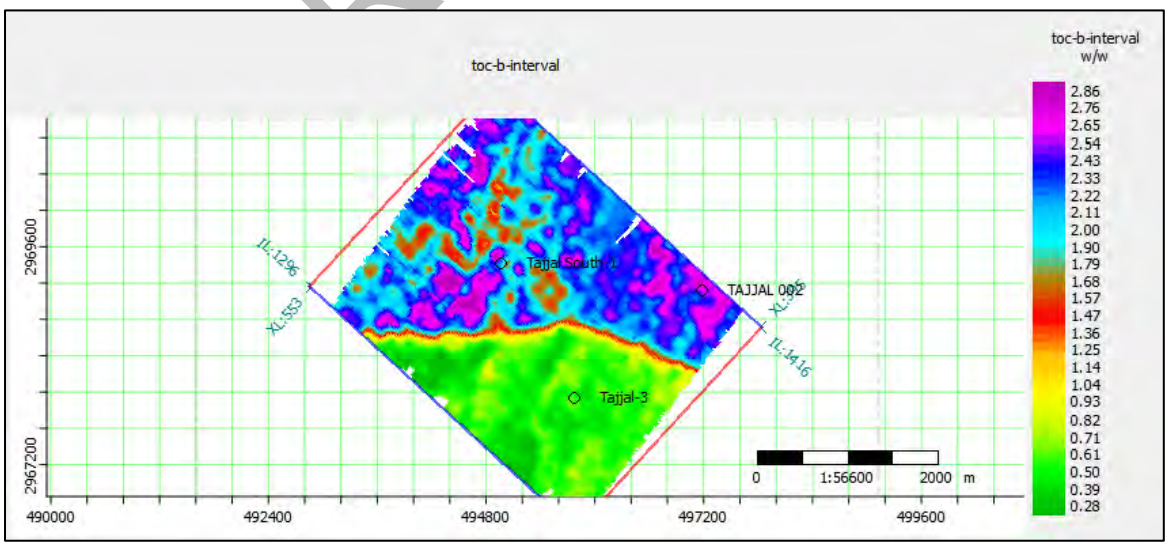

Figure 5.15. Data slice at B-Sand Interval shows the variation of TOC across the survey.

The results of neural network correlation between the seismic and targeted logs are applied on the 3D volume as shown in Figure 5.13 and 5.14. Figure 5.16 shows data slice of computed TOC at B-Sand Interval with the average value of 0.5 wt. % at Tajjal-03 and 2.6 wt. % at Tajjal-02.

CONCLUSIONS

1. Structural interpretation confirm the presence of an extensional regime. Seven normal faults are present on seismic data with faults F2, F5, F6 and F7 forming horst and graben structures.
2. Source rock evaluation of B- Sand Interval within Tajjal-03 and Tajjal-02 wells confirms that it has the potential to act as unconventional source. Shale play identification shows 1.2-2.5 wt. % TOC in targeted zone of Tajjal-02 lying in fair source generation potential window and 0.2-1.5 wt. % TOC in targeted zone of Tajjal-03 which lies in the realm of very poor to poor source generation potential window.
3. The seismic inversion and log data were successfully used in integrated research to determine the "Total Organic Carbon" of B-Sand Interval. Consistent results of acoustic impedance were calculated using linear programming sparse spike inversion with the correlation coefficient 0.99 and root mean square error of 0.04% respectively. Average spatial TOC value evaluated with the model-based inversion is approximately 0.5 wt. % at Tajjal-03 and surrounding area whereas 2.6 wt.% TOC is calculated at Tajjal-02 and its vicinity marking this zone in B-Sand Interval as fair source potential window.

REFERENCES

Abbas, S. T., Mirza, K., & Arif, S. J. (2015). Lower Goru formation-3D modeling and petrophysical interpretation of Sawan Gas field, Lower Indus basin, Pakistan. *The Nucleus*, *52*(3), 138-145.

Abbasi, S. A. An Integrated Study to Analyze TheReservoir Potential Using Stochastic Inversion, Model Based Inversion 1 and Petrophysical Analysis: A Case Study From The Southern Indus Basin, Pakistan 2.

Ahmad, A., Ahmad, N., Wali, N., & Manshoor, S. A. (2007). Source potential and maturity trends of Lower Permian sediments in the Punjab platform and adjoining areas, Pakistan. In *Annual Technical Conference, Pakistan, Proceedings* (pp. 139-154).

Ahmad, N., & Khan, M. (2010). Play fairway analysis and CRS mapping within a Sequence Stratigraphic Framework: screening tools for geological risk constrained exploration. In *PAPG-SPE Annual Technical Conference*.

Alexander, T., Baihly, J., Boyer, C., Clark, B., Waters, G., Jochen, V., Calvez, J.L., Lewis, R., Miller, C.K., Thaeler, J., & Toelle, B. E. (2011). Gas shale revolution. *Oilfield rev*, *23*, 40-55.

Ali, A., Alves, T. M., Saad, F. A., Ullah, M., Toqeer, M., & Hussain, M. (2018). Resource potential of gas reservoirs in South Pakistan and adjacent Indian subcontinent revealed by post-stack inversion techniques. *Journal of Natural Gas Science and Engineering*, *49*, 41-55.

Ali, M., Khan, M. J., Ali, M., & Iftikhar, S. (2019). Petrophysical analysis of well logs for reservoir evaluation: a case study of "Kadanwari" gas field, middle Indus basin, Pakistan. *Arabian Journal of Geosciences*, *12*(6), 1-12.

Alshakhs, M., & Rezaee, M. R. (2017). A new method to estimate total organic carbon (TOC)

content, an example from goldwyer shale formation, the canning basin. *The Open Petroleum Engineering Journal*, *10*, 118-133.

Bakker, P. (2002). *Image structure analysis for seismic interpretation* (pp. 32-34).

Barclay, F., Bruun, A., Rasmussen, K. B., Alfaro, J. C., Cooke, A., Cooke, D., ... & Roberts, R. (2008). Seismic inversion: Reading between the lines. *Oilfield Review*, *20*(1), 42-63.

Beers, R. F. (1945). Radioactivity and organic content of some Paleozoic shales. *AAPG Bulletin*, *29*(1), 1-22.

Blyth, F. G. H., & De Freitas, M. H. (1987*). A Geology for engineers.*

Broadhead, M. K., Cheshire, S. G., & Hayton, S. (2016). The effect of TOC on acoustic impedance for a Middle Eastern source rock. *The Leading Edge,* 35(3), 258-264.

Brohi, I. A., Solangi, S. H., Abbasi, S. A., Bablani, S. A., Khokhar, Q. D., Sahito, A. G., & Brohi, A. U. (2013). Joint analysis and economic significance of Lakhra Formation in the vicinity of Khanu Brohi, Jamshoro, Sindh. *Sindh University Research Journal-SURJ (Science Series)*, *45*(2).

Caineng, Z., Guangya, Z., Shizhen, T., Suyun, H., Xiaodi, L., Jianzhong, L., & Xinjing, L. (2010). Geological features, major discoveries and unconventional petroleum geology in the global petroleum exploration. *Petroleum Exploration and Development*, *37*(2), 129-145.

Coffeen, J. A. (1978). Seismic exploration fundamentals.

Dellenbach, J. (1983). Source rock logging.

Dobrin, M. B., & Savit, C. H. (1960). *Introduction to geophysical prospecting* (Vol. 4). New York: McGraw-hill.

Durand, B., & Nicaise, G. (1980). *Kerogen: Insoluble organic matter from sedimentary rocks*. Editions technip.

EIA, E. (2013). ARI World Shale Gas and Shale Oil Resource Assessment Technically Recoverable Shale Gas and Shale Oil Resources: An Assessment of 137 Shale Formations in 41 Countries outside the United States. *Washington DC: US Energy Information Administration*.

Farah, A., Abbas, G., De Jong, K. A., & Lawrence, R. D. (1984). Evolution of the lithosphere in Pakistan. *Tectonophysics*, *105*(1-4), 207-227.

Herron, S., Letendre, L., & Dufour, M. (1988). Source rock evaluation using geochemical information from wireline logs and cores. *AAPG Bull.; (United States)*, *72*(CONF-8809346-).

Holmes, M., Holmes, D., & Holmes, A. (2011, July). A petrophysical model to estimate free gas in organic shales. In *Annual Conference and Exhibition, Houston, Texas, AAPG Search and Discovery Article* (Vol. 40781).

Hussain, M., Chun, W. Y., Khalid, P., Ahmed, N., & Mahmood, A. (2017). Improving petrophysical analysis and rock physics parameters estimation through statistical analysis of Basal sands, Lower Indus Basin, Pakistan. *Arabian Journal for Science and Engineering*, *42*(1), 327-337.

Kadri, I. B. (1995). *Petroleum geology of Pakistan*. Pakistan Petroleum Limited.

Karbalaali, H., Shadizadeh, S. R., & Riahi, M. A. (2013). Delineating hydrocarbon bearing zones using elastic impedance inversion: A Persian Gulf example. *Iranian Journal of Oil and Gas Science and Technology*, *2*(2), 8-19.

Kazmi, A. H., & Jan, M. Q. (1997). *Geology and tectonics of Pakistan*. Graphic publishers.

Kazmi, A. H., & Abbasi, I. A. (2008). *Stratigraphy & historical geology of Pakistan* (p. 524). Peshawar, Pakistan: Department & National Centre of Excellence in Geology.

Kelishami, S. B. A., Mohebian, R., & Salmian, O. (2022). A comprehensive perspective on pore

connectivity and natural fracture analysis in Oligo-Miocene heterogeneous carbonates, southern Iran. *Journal of Petroleum Science and Engineering*, *208*, 109199

Khalid, P., Ehsan, M. I., Akram, S., Din, Z. U., & Ghazi, S. (2018). Integrated reservoir characterization and petrophysical analysis of cretaceous sands in Lower Indus Basin, Pakistan. *Journal of the Geological Society of India*, *92*(4), 465-470.

Landais, P. (1997). Petroleum Geochemistry and Geology, Edited by John M. Hunt, WH Freeman, et al. 1996. ISBN 0-7167-2441-3. 743 pp.

Mahmud, S. A., & Sheikh, S. A. (2009, November). Reservoir potential of lower nari sandstones (Early Oligocene) in southern Indus basin and Indus offshore. In *Annual Technical Conference (ATC)* (pp. 7-8).

Majid, K., Shahid, N., Munawar, S., & Muhammad, H. (2016). Interpreting Seismic Profiles in terms of Structure and Stratigraphy with Implications for Hydrocarbons Accumulation, an Example from Lower Indus Basin Pakistan. *Journal of Geology & Geophysics*, *5*(5), 1-9.

Maurya, S. P., & Sarkar, P. (2016). Comparison of post stack seismic inversion methods: a case study from Blackfoot Field, Canada. *International Journal of Scientific and Engineering Research*, *7*(8), 1091-101.

Meyer, B. L., & Nederlof, M. H. (1984). Identification of source rocks on wireline logs by density/resistivity and sonic transit time/resistivity crossplots. *AAPG bulletin*, *68*(2), 121-129.

Naeem, M., Jafri, M. K., Moustafa, S. S., AL-Arifi, N. S., Asim, S., Khan, F., & Ahmed, N. (2016). Seismic and well log driven structural and petrophysical analysis of the Lower Goru Formation in the Lower Indus Basin, Pakistan. *Geosciences Journal*, *20*(1), 57-75.

Naseer, M. T., Asim, S., & ABBASI, S. (2016). Spectral Decomposition and Seismic Attributes for Clastic Reservoir Analysis of Miano Gas Field, Southern Indus Basin, Pakistan. *Sindh University Research Journal-SURJ (Science Series)*, *47*(1).

Passey, Q. R., Creaney, S., Kulla, J. B., Moretti, F. J., & Stroud, J. D. (1990). A practical model for organic richness from porosity and resistivity logs. *AAPG bulletin*, *74*(12), 1777-1794.

Pendrel, J. (2001). Seismic inversion—The best tool for reservoir characterization. *CSEG Recorder*, *26*(1), 18-24.

Peters, K. E., & Cassa, M. R. (1994). Applied source rock geochemistry: Chapter 5: Part II. Essential elements.

Pico, A., & Salinas, T. (2017). Shale volume estimation using seismic inversion and multiattributes for the characterization of a thin sand reservoir in the llanos Basin, Colombia. In *SEG Technical Program Expanded Abstracts 2017* (pp. 2034-2038). Society of Exploration Geophysicists.

Prasad, M., Mba, K. C., McEvoy, T. E., & Batzle, M. L. (2011). Maturity and impedance analysis of organic-rich shales. *SPE Reservoir Evaluation & Engineering*, *14*(05), 533-543.

Qayyum, F., Hanif, M., Mujtaba, M., Wahid, S., & Ali, F. (2016). Evaluation of source rocks using one dimensional maturity modeling in Lower Indus Basin, Pakistan. *Arabian Journal of Geosciences*, *9*(4), 1-22.

Raza, H. A., Ali, S. M., & Ahmed, R. (1990). Petroleum geology of Kirthar sub-basin and part of Kutch Basin. *Pakistan Journal of Hydrocarbon Research*, *2*(1), 27-73.

Rider, M., & Kennedy, M. (2002). The geological interpretation of well logs: Sutherland. *Scotland, Rider-French Consulting Ltd*.

Schmoker, J. W. (1979). Determination of organic content of Appalachian Devonian shales from formation-density logs: Geologic notes. *AAPG Bulletin*, 63(9), 1504-1509.

Schmoker, J. W., & Hester, T. C. (1989). Oil Generation Inferrred From Formation Resistivity--Bakken Formation, Williston Basin, North Dakota. In *SPWLA 30th Annual Logging Symposium*. OnePetro.

Schmoker, J. W., & Hester, T. C. (1989). Oil generation inferred from formation resistivity—Bakken Formation. In *Williston basin, North Dakota: Transactions of the Thirtieth SPWLA Annual Logging Symposium, paper H*.

Sheikh, N., & Giao, P. H. (2017). Evaluation of shale gas potential in the lower cretaceous Sembar formation, the southern Indus basin, Pakistan. *Journal of natural gas science and engineering*, *44*, 162-176.

Siyar, S. M., Waqas, M., Mehmood, S., Jan, A., Awais, M., & Islam, F. (2017). Petrophysical characteristics of lower Goru formation (Cretaceous) in Sawan gas field, central Indus basin, Pakistan. *Journal of Biodiversity and Environmental Sciences (JBES)*, *10*(5), 260-266.

Sohail, G. M., Hawkes, C. D., & Yasin, Q. (2020). An integrated petrophysical and geomechanical characterization of Sembar Shale in the Lower Indus Basin, Pakistan, using well logs and seismic data. *Journal of Natural Gas Science and Engineering*, *78*, 103327.

Sunjay. (2011). Shale gas exploration and production. In *12th International Congress of the Brazilian Geophysical Society & EXPOGEF, Rio de Janeiro, Brazil, 15–18 August 2011* (pp. 1432-1435). Society of Exploration Geophysicists and Brazilian Geophysical Society.

Swanson, V. E. (1960). *Oil yield and uranium content of black shales* (No. TID-27491). Geological Survey, Washington, DC (USA).

Tissot, B. P., & Welte, D. H. (1978). Sedimentary processes and the accumulation of organic matter. In *Petroleum Formation and Occurrence* (pp. 55-62). Springer, Berlin, Heidelberg.

Welte, D. H., & Tissot, P. B. (1984). *Petroleum formation and occurrence*. Springer-verlag.

Veeken, P. C. H., & Da Silva, A. M. (2004). Seismic inversion methods and some of their constraints. *First break*, *22*(6).

Zaigham, N. A., & Mallick, K. A. (2000). Prospect of hydrocarbon associated with fossil-rift

structures of the southern Indus basin, Pakistan. *AAPG bulletin*, *84*(11), 1833-1848.

www.ppl.com.pk.